Background

Protein ubiquitination plays a crucial role in numerous cellular processes such as cell growth, regulation of diverse signal transduction and disease [1-3]. The covalent attachment of ubiquitin to protein substrates requires a stepwise cascade of enzymatic reactions. First, ubiquitin is activated by E1 (ubiquitin-activating enzyme, UBA) in an ATP-dependent manner by forming a high-energy thioester-bond between the carboxyl-terminal glycine residue of ubiquitin and a cysteine residue of E1. The activated ubiquitin is then transferred to the core-cysteine residue of E2 (ubiquitin-conjugating enzyme, UBC). Together with an E3 ligase enzyme, ubiquitin is attached via its carboxyl-terminus to an e-amino group of a lysine residue in the target protein. Since E3 binds to both E2 and the target protein, and acts as scaffold between E2 and the substrate protein, the E3 ligase is the major determinant for selecting target proteins for ubiquitination. There is large number of genes encoding E3 ligases in all eukaryotes, and the diversity of E3s is thought to contribute to the substrate specificity of numerous target proteins. E3 ligases are structurally divided into three groups: HECT, RING and U-box [4]. The HECT-type E3 ligase is distinct from the other two ligases in that it forms a thioester-bond with ubiquitin prior to the transfer of ubiquitin to target proteins. The RING-type E3 ligase contains a unique domain similar to the zinc finger motif that mediates protein-protein interactions [5] and is further divided into two classes: one that can function alone and another that forms a complex with other E3 components [4].

Recent studies have shown that attachment of polyubiquitin chains on target proteins linked via lysine-48 of ubiquitin typically leads to degradation by the 26S proteasome [6], whereas linkage via lysine-63 mediates different pathways such as internalization of membrane proteins, activation of signal transduction and DNA damage repair [7]. The formation of lysyl-63-linked polyubiquitin chains is generated by specific combinations of E2s and E2 variants, which are similar to E2s except that they lack core cysteine residues required for E2 activity [8,9]. In addition, ubiquitination of substrates without polymerization, mono-ubiquitination, acts as a sorting signal for protein endocytosis and as a regulation factor for diverse proteins, including histones and transcription factors [10].

In plant, genomic research of the model plant *Arabidopsis thaliana* showed that there are two E1s, 37 E2s and more than 1,300 predicted E3s [11]. Although little is known about protein ubiquitination in plants compared with yeast and mammals, recent studies revealed that the plant ubiquitination pathway is involved in the regulation of morphogenesis, the circadian clock and responding to hormone or pathogen signal molecules [12-15]. Despite the importance of ubiquitination in plants, much of the plant ubiquitination cascade is still unknown because of its complexity and the issues inherent to the use of Arabidopsis plants for biochemical analysis. Although several interactions between E2s and RING type E3s have been demonstrated *in vitro* using recombinant proteins expressed in *Escherichia coli*, these efforts are hampered by the inability to obtain functional protein using conventional methods [16].

With this in mind, we sought to develop a novel *in vitro* method to analyze the ubiquitin pathway genome-wide. The two major obstacles hindering the development of an *in vitro* assay for genome-wide screening are the difficulty of efficiently producing recombinant protein and the inability to detect ubiquitination in a high-throughput fashion. To address the first problem we used the wheat cell-free protein synthesis system, which has been previously reported to produce a wide range of functional Arabidopsis and human proteins [17-19]. Moreover, a collection of RIKEN Arabidopsis Full Length (RAFL) cDNA clones covering about 70% of Arabidopsis genes is available [20]. Using these RAFL clones as templates, recombinant proteins involved in the ubiquitination pathway were expressed in the wheat cell-free system and used for several functional analyses. For screening, conventional detection methods such as immunoblot analysis or radioisotope-labeled proteins are not suitable for the detection of a large number of ubiquitination reactions. Recently, a high-throughput luminescence method to detect protein ubiquitination was reported [21], however this method requires purified protein and creation of specialized vectors to produce proteins. In this study, a novel *in vitro* assay to detect polyubiquitin chain formation was developed using wheat cell-free synthesis and a modified luminescence-based detection method. We demonstrate (1) creation of a simple *in vitro* method to detect polyubiquitination using crude recombinant E3s, (2) discovery of the activity of At1g55530 by screening a RING subgroup in the reported assay, and (3) the polyubiquitination assay in the presence of MG132 demonstrated the absence of 26S proteasome-dependent protein degradation activity in wheat cell-free system.

Results

Detection of Polyubiquitin Chains on AtUBC22 E2 enzyme

Recently, AtUBC22 (At5g05080) E2 protein has been shown to catalyze polyubiquitin chain formation without an E3 ligase, although AtUBC35 (At1g78870) E3-independent polyubiquitination activity could not be detected [16]. We employed AtUBC22 and AtUBC35 as model E2 proteins to develop a novel polyubiquitination assay. We have also demonstrated that addition of biotin ligase (BirA) and biotin to the wheat cell-free protein production system yields a single biotinylation on a target pro-

tein containing a biotin ligation site [22]. Using this method, biotinylated recombinant AtUBC22 and AtUBC35 were synthesized and, without purification from the translation mixture, the polyubiquitination reaction was performed on the crude recombinant protein. After the reaction, biotinylated AtUBC22 and AtUBC35 were purified using streptavidin-conjugated magnetic beads and the polyubiquitin chain was detected by immunoblot analysis. As shown in Fig 1A, AtUBC22 showed polyubiquitination, whereas AtUBC35 showed mainly monoubiquitination. Interestingly, both E2s still had activity in absence of exogenous E1 in polyubiquitin reaction mixture (Fig. 1A, middle lanes), suggesting that wheat cell-free system has high endogenous E1 activity.

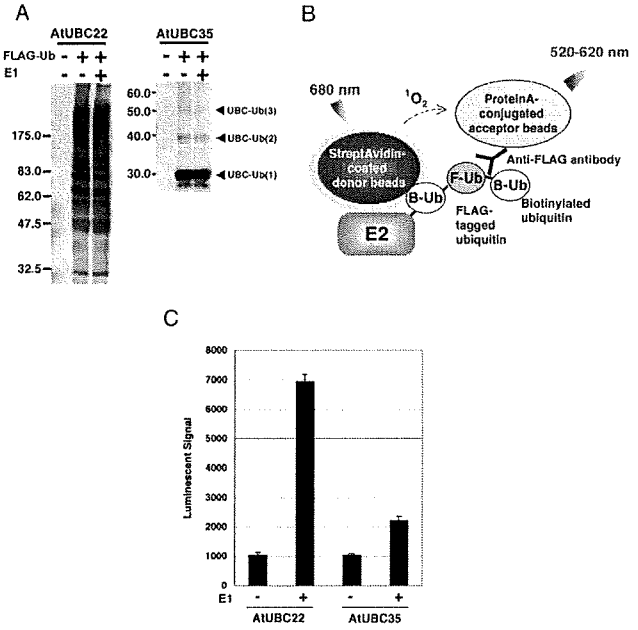

Figure 1
Detection of E3-independent polyubiquitination of AtUBC22 by luminescent analysis. A, Polyubiquitin chain on AtUBC22 but not on AtUBC35 was detected by immunoblot analysis. In this assay, polyubiquitination reaction was carried out with FLAG-tagged ubiquitin, and detected by immunoblot analysis using anti-FLAG antibody. B, Schematic diagram of detection of polyubiquitin chains by luminescent analysis. Protein A-conjugated acceptor beads and streptavidin-coated donor beads are bound to anti-FLAG antibody bound to FLAG-tagged ubiquitin and biotinylated E2, respectively, and these two beads are in closed proximity when polyubiquitin chain formed. Upon excitation 680 nm, a singlet oxygen is generated from the donor beads, and then transferred to the acceptor beads within 200 nm, and the singlet oxygen reacts the acceptor beads which in turn emits light at 520–620 nm. This light is measured by AlphaScreen kit and change to signal value. C, Polyubiquitin chain on purified recombinant E2 was detected by luminescent analysis in the presence (E1 +) or absence (E1 -) of exogenous E1. Error bars represent standard deviations from three independent experiments.

While immunoblot analysis is an excellent detection method, it is not suitable for high-throughput detection of numerous polyubiquitination reactions. Initially, we attempted to use luminescent analysis, based on the AlphaScreen technology, to detect the polyubiquitination activity of AtUBC22 and AtUBC35. In principle, if a polyubiquitin chain is formed by FLAG-tagged and biotinylated ubiquitins, it will bring into proximity the streptavidin-coated donor bead (bound to biotin) and the protein A-conjugated acceptor bead (bound to anti-FLAG IgG), producing a luminescent signal (Fig. 1B). Considering that the wheat cell-free system has high endogenous E1 activity (Fig. 1A), it may also have endogenous E2 and E3 activity. In order to avoid formation of polyubiquitin chains by an endogenous wheat germ ubiquitin pathway, purified E2s were used in this assay. As shown in Fig 1C, high luminescent signal was observed in the presence of AtUBC22 in E1-dependent manner. In contrast, AtUBC35 showed low signal. The two luminescent signals were approximately consistent with immunoblot data that AtUBC22 and AtUBC35 have high and low polyubiquitination activities respectively, as demonstrated in Fig 1A. These results indicate that the luminescent method can detect polyubiquitin chain formation by using the two types of ubiquitins.

Ubiquitination and Polyubiquitination Analyses of HECT-TypeE3 Ligases

Polyubiquitination activity of E3 ligases activated by the step-wise E1 to E3 cascade is well documented [3]. We next attempted to reconstruct this cascade *in vitro* and to detect the E3-formed polyubiquitin chains using our luminescent method. Due to the size of HECT-type E3 ligases, ranging from 100 to 428 kDa in Arabidopsis, production of active protein by traditional expression methods may not be easy and biochemical analysis using only truncated recombinant protein has been carried out previously [23]. We attempted to produce full-length Arabidopsis HECT-type E3 ligase proteins using the wheat cell-free system and monitored ubiquitin-conjugation and polyubiquitination by luminescence. Two genes that encode Arabidopsis HECT-type E3 ligase, *UPL5* and *UPL7* [24], were analyzed in this study. We obtained UPL5 and UPL7 cDNA from the RAFL library and produced FLAG-tagged protein in the wheat cell-free system. Ubiquitination of FLAG-labeled UPLs (UPL-FLAGs) was investigated by both the luminescent and immunoblot methods. The successful production of the two recombinant HECT proteins was observed by immunoblot analysis (Fig. 2A) and used in the luminescence assay without purification. To detect ubiquitination of the HECT proteins, UPL-FLAGs

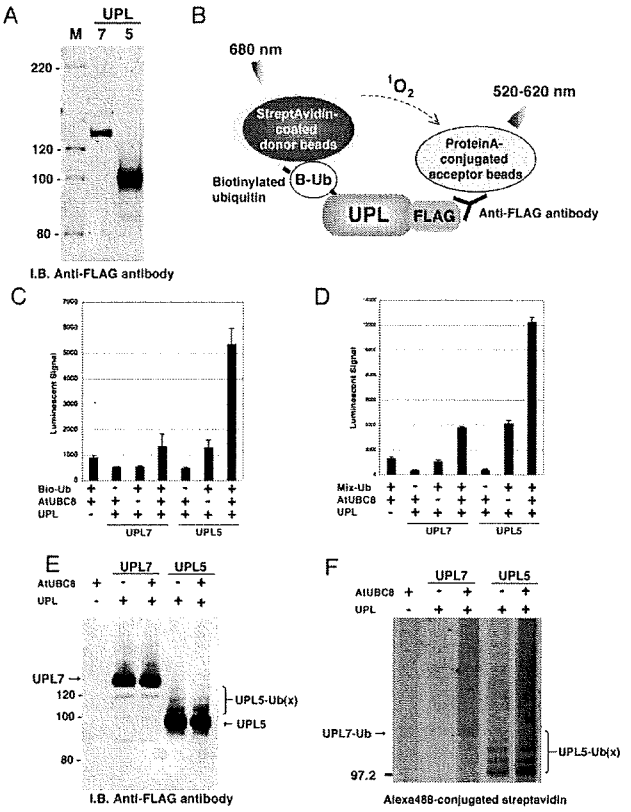

Figure 2

Analysis of recombinant Arabidopsis HECT-type E3 ligases (UPL7 and UPL5). A, Production of FLAG-tagged recombinant UPL proteins was detected by immunoblot analysis. For analysis, 5 μl of crude recombinant UPL proteins were loaded, and detected by immunoblot analysis using anti-FLAG antibody. B, Schematic diagram of detection of ubiquitin-conjugation of UPLs by luminescent analysis. Protein A-conjugated acceptor beads and streptavidin-coated donor beads were bound to anti-FLAG antibody bound to FLAG-tagged recombinant UPLs and biotinylated ubiquitin, respectively, and detected by same principle and procedure described in Figure 1B. C, The ubiquitination of crude recombinant UPL7 and UPL5 was detected by luminescent analysis described in B. Bio-Ub means biotinylated ubiquitin. D, polyubiquitination of crude recombinant UPL7 and UPL5 was detected by luminescent analysis with anti-His antibody. Mix-Ub indicated the mixture of His-tagged and biotinylated ubiquitin. E and F, Mobility shift of UPLs (E) and formation of polyubiquitin chains (F) were detected by immunoblot using anti-FLAG antibody and Alexa488-conjugated streptavidin, respectively. The polyubiquitination reaction was done with FLAG-tagged recombinant UPLs in presence or absence of crude AtUBC8, and then recombinant UPLs were purified by anti-FLAG antibody-conjugated agarose. Error bars represent standard deviations from three independent experiments.

and biotinylated ubiquitin were used. When biotinylated ubiquitin is conjugated to the UPL-FLAG, a high luminescent signal is obtained (Fig. 2B). As a result of the analysis, ubiquitin-conjugation of UPL5 was observed (Fig. 2C). In addition, polyubiquitin chains formed by UPLs were detected with the luminescence assay using His-tagged and biotinylated ubiquitin. To subtract polyubiquitin chain formation from endogenous E2 and E3 in wheat cell-free system, the assay was performed without recombinant UPL and only low signal was detected (Fig. 2D, "UPL-" lane). As expected, luminescent signal was observed in recombinant UPL5 and UPL7 (Fig. 2D). Although the luminescent signal of UPL7 was lower than that of UPL5, the signal was still two-fold higher than the endogenous background signal. These results were confirmed by immunoblot analysis that showed distinct mobility shifts of UPL5 (Fig. 2E) when detecting FLAG-tagged UPLs, and polyubiquitin chain formation of UPL5 monitoring Alexa488-conjugated streptavidin (Fig. 2F). Comparing the amount of polyubiquitin chain formation in absence of UPLs (Fig. 2F, "UPL-" lane), UPL7 formed weak but distinct polyubiquitin chains in presence of AtUBC8. These luminescent signals were consistent with immunoblot data. Interestingly, polyubiquitin chains were formed by UPL5 without supplementing exogenous E2 protein (Fig. 2D and 2F, "AtUBC8-" lane), suggesting that wheat germ extract has endogenous E2 activity as well as endogenous E1 activity. These data indicate that the wheat cell-free production system is able to produce high molecular weight proteins in functional forms and that our luminescence method can detect activity of HECT-type E3 ligases without purification. This is the first data showing that full length recombinant HECT-type E3s have ubiquitin-conjugating and polyubiquitination activity. Taken together, the luminescent method based on the wheat cell-free system could be useful for biochemical analysis of HECT-type E3 ligases.

Detection of Polyubiquitin Chains by RING-Type CIP8 E3 Ligase

It is reported that at least 469 predicted RING-type E3 ligases are encoded in the Arabidopsis genome [25]. Like the HECT-type E3, we attempted to express and carry out the functional analysis of the RING-type E3 ligases. In this study, we selected CIP8 as a model RING-type E3 ligase, which is reported to possess a RING finger motif and have typical features of an E3 ligase [26]. At first, polyubiquitination activity of purified CIP8 in presence or absence of exogenous E1 and purified E2 (AtUBC8) was investigated by luminescence. As shown in Fig 3A, luminescence analysis using His-tagged and biotinylated ubiquitin showed the polyubiquitination of purified CIP8 only when exogenous E1 and purified E2 were added to the reaction mixture. The CIP8-dependent polyubiquitination was

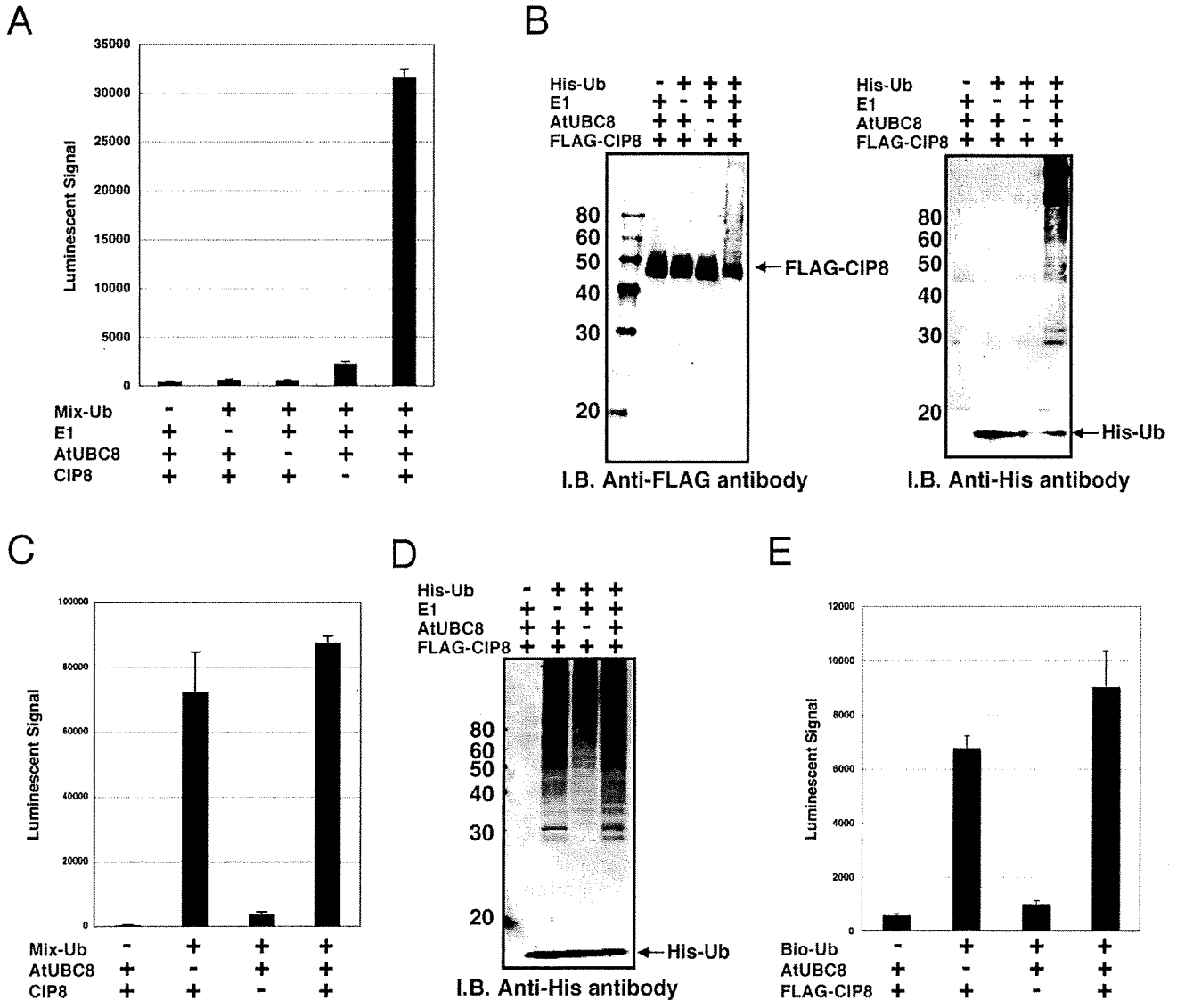

Figure 3

Detection of polyubiquitination and self-ubiquitination of CIP8. A to D, The polyubiquitination assay was carried out with purified (A and B) or crude recombinant CIP8 (C and D) and detected by luminescent analysis with anti-FLAG antibody (A and C) and immunoblot analysis (B and D). His-Ub or Mix-Ub indicate His-tagged ubiquitin or the mixture of FLAG-tagged and biotinylated ubiquitin, respectively. The polyubiquitination assay using luminescent analysis was carried out with recombinant CIP8 without tag in the presence or absence of ubiquitin related components indicated below each graph. E, Ubiquitination of crude recombinant CIP8 was observed by luminescent analysis with anti-FLAG antibody. The assay was carried out with or without biotinylated ubiquitin and crude AtUBC8 recombinant protein. Bio-Ub means biotinylated ubiquitin. Error bars represent standard deviations from three independent experiments.

confirmed by immunoblot analyses detecting both FLAG-CIP8 and His-tagged ubiquitin (Fig. 3B). On the other hand, luminescent analysis with crude CIP8 protein showed high polyubiquitination activity both in the presence or absence of purified E2 (Fig. 3C), and was confirmed by immunoblot analysis with crude protein (Fig. 3D). These data indicated that, like recombinant UPL5, crude CIP8 also utilized endogenous wheat extract E1 and E2 proteins, and therefore we could carry out the simple polyubiquitination analysis of E3 without addition of exogenous E1 and E2 proteins. Furthermore, immunoblot analysis detecting purified CIP8 (Fig. 3B) showed a mobility shift of FLAG-tagged CIP8 to higher molecular weights due to ubiquitination, whereas the mobility of the E2 was

not altered (data not shown). This result indicates that the CIP8-dependent polyubiquitin chains might be elongated on CIP8 itself. This data is consistent with a recent report showing that TRIM5a, a typical RING-type E3 ligase in human, also undergoes self-ubiquitination, forming polyubiquitin chains on itself [27]. To clarify whether the mobility shift of CIP8 was concomitant with polyubiquitin chain formation resulting from self-ubiquitination, we tried to detect ubiquitination of CIP8 by the luminescent method using crude FLAG-CIP8 protein and biotinylated ubiquitin. The luminescent method clearly detected the binding of biotinylated ubiquitin to FLAG-tagged CIP8 both in the presence and absence of exogenous E2 (Fig. 3E). Similar to polyubiquitin formation, the ubiquitination of CIP8 also occurred without the addition of exogenous E2 protein (Fig. 3E, "AtUBC8-" lane). Taken together, these data demonstrate that the luminescent method could detect formation of RING-type CIP8-dependent polyubiquitin chains and self-ubiquitination of crude CIP8.

Screening of RING-Type E3 Ligases Having Polyubiquitination Activity

Recent papers have reported that the polyubiquitin chain is an important biological regulator. Identification of activity and features of E3 ligases offers important information about the ubiquitin-dependent regulation system. Our luminescent method based on the wheat cell-free system produced a simple and high-sensitivity detection of CIP8-dependent polyubiquitin chains without any purification (Fig. 3C). Using these tools, we screened new E3 ligases for the ability to form polyubiquitin chains like CIP8.

The RING-type E3 ligases in Arabidopsis were divided into 30 subgroups based on domain structure, and CIP8 is categorized into subgroup 6 as it contains a coiled-coil domain [25]. Eight other RING-type E3s from subgroup 6 were selected for screening, and the simple polyubiquitination assay was carried out with FLAG-tagged and biotinylated ubiquitins, and the crude recombinant RING-type E3s without addition of exogenous E1 and E2. The screening result showed significant polyubiquitination activity of At1g55530, whereas other RING-E3 proteins were not active (Fig. 4A). Immunoblot analysis of purified recombinant At1g55530 confirmed the polyubiquitination activity and indicated that At1g55530 was self-ubiquitinated (Fig. 4B). The polyubiquitination activity of At1g55530 suggests that it may have a biological role for proteasome-mediated degradation like CIP8 [26]. These results show that the wheat cell-free protein expression system and the luminescent ubiquitination detection method could support functional high-throughput screening of E3 proteins.

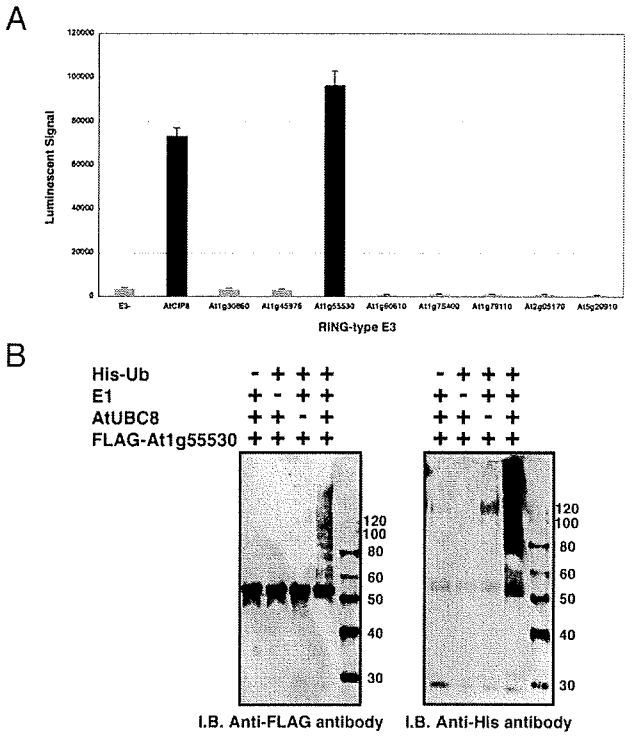

Figure 4
Screening of RING-type E3 ligases having polyubiquitination activity. A, Polyubiquitination reaction of crude recombinant E3 proteins was carried out with mixture of FLAG-tagged and biotinylated ubiquitins, and investigated by luminescent analysis with anti-FLAG antibody. B, Polyubiquitination activity of At1g55530 was confirmed by immunoblot analysis. The assay was carried out using purified recombinant AtUBC8 and At1g55530, and mobility shift of FLAG-tagged At1g55530 and polymer of His-ubiquitin were detected by immunoblot analysis using anti-FLAG and anti-His antibodies, respectively. Error bars represent standard deviations from three independent experiments.

Analysis of the Wheat Cell-free Based Ubiquitination in the Presence of Proteasome Inhibitor

It is known that some cell extracts, such as rabbit reticulocyte or HeLa S-100 fraction, have 26S proteasome-dependent proteolytic activity [28,29]. Based on the presence of endogenous E1 and E2 ubiquitination and polyubiquitination in the wheat cell-free system, it is expected that the 26S proteasome activity will be very low (Fig. 2, 3 and 4). It was previously reported that the wheat germ extract had little 26S proteasome-dependent protein degradation activity [30]. Thus, we determined whether the wheat cell-free system contains active 26S proteasome. Using the crude recombinant proteins that formed polyubiquitin chains in this study, the polyubiquitination reaction was carried out in presence or absence of MG132, and accrual of the polyubiquitinated recombinant pro-

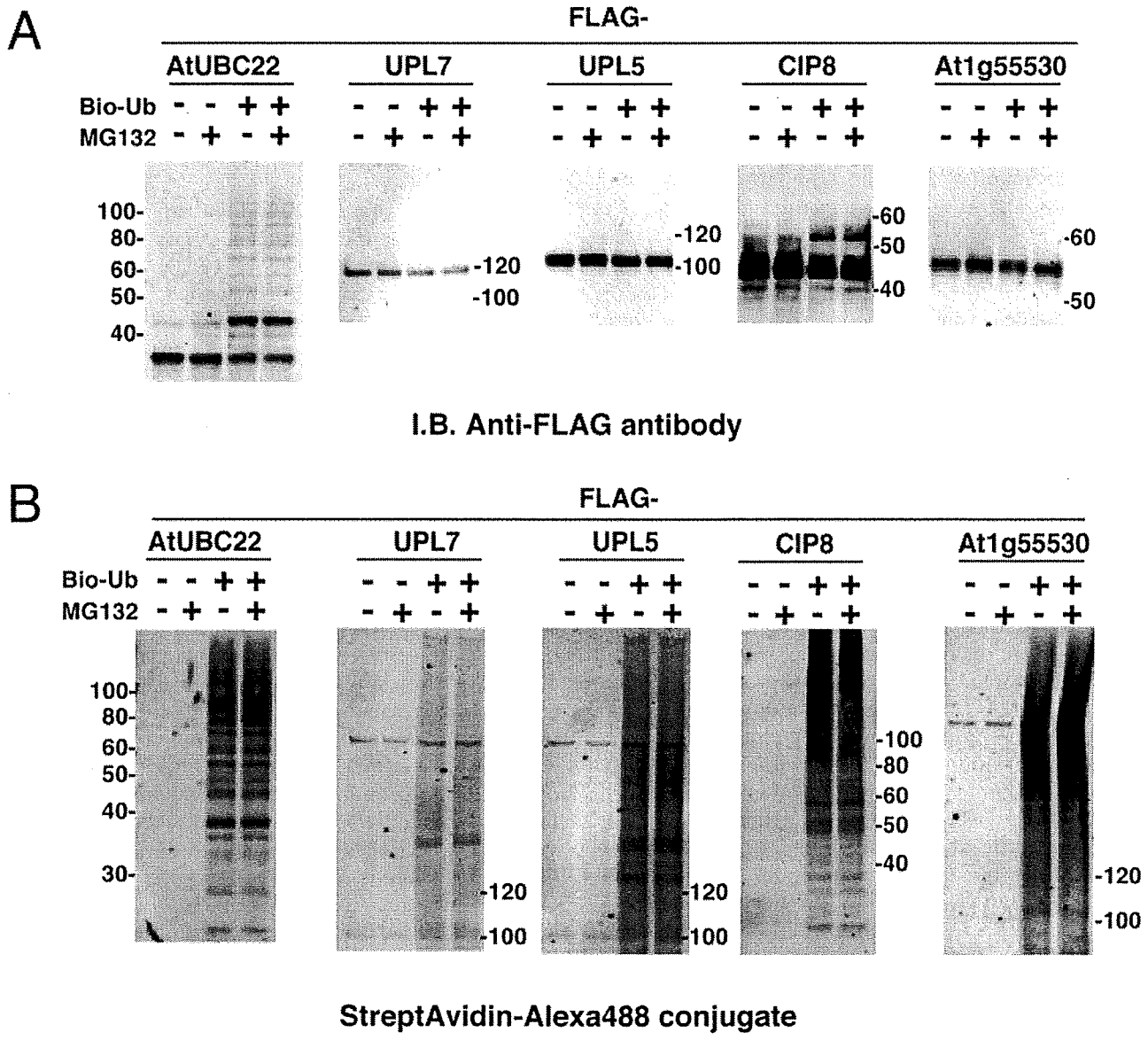

Figure 5
Effect of proteasome inhibitor on stability of polyubiquitinated proteins. Polyubiquitination assays of crude FLAG-tagged E2s and E3s were carried out in the presence or absence of biotinylated ubiquitin and 20 μM MG132. A, FLAG-tagged recombinant proteins were detected by immunoblot analysis using anti-FLAG antibody. B, Polyubiquitination chain formed by each recombinant protein was detected by Alexa488-conjugated streptavidin.

teins and its polyubiquitin chain was estimated. As shown in Fig 5, the amounts of UBC22, UPL5, UPL7 and At1g55530 (Fig. 5A) and of its polyubiquitin chains (Fig. 5B) were hardly altered by MG132 treatment. This result indicates that the proteolytic activity of the 26S proteasome in the wheat cell-free system was below the detection level. Thus, the wheat cell-free system could be suitable for ubiquitination analysis.

Discussion

The ubiquitin signal is an important protein modification in eukaryotes. Binding of a single ubiquitin to a target protein, mono-ubiquitination, is essential for membrane trafficking, protein functions and protein-protein interaction [7]. As for polyubiquitination, both Lys-48- and Lys-63-linked polyubiquitin chains have been well characterized in mammals and yeast. Lys-48 linked chains cause proteolysis of target proteins [6], and Lys-63 linked chains reg-

ulate signal transduction such as cellular localization of protein or protein-protein interactions [7]. In mammals, the multi-functional activities of NF-κB are regulated by the Lys-63 linked chain [31]. In plants, the function of the Lys-63 linked chain is still obscure. However, Arabidopsis E2 and its variants promote formation of the Lys-63 linked chain [32], suggesting that the Lys-63 linked chain in plant cells might also function similar to animal cells. Hence, comprehensive analysis of the ubiquitin-related plant proteins would open a door for elucidation of the plant ubiquitin pathway. In this study, we developed a simple and highly sensitive ubiquitination assay method by combination of the wheat cell-free protein synthesis system and luminescent detection. In general, *in vivo* protein production requires many time-consuming steps such as vector construction, cell culture and purification to obtain the recombinant protein. In contrast, this cell-free based luminescence method could analyze a large amount of ubiquitin reactions without these steps.

Using this method, we conveniently detected polyubiquitin chain formation of E2 and E3s by using two tagged ubiquitins (Fig. 1, 2, 3 and 4). The result of polyubiquitination analysis of the E2s obtained from luminescent-based detection method was verified by immunoblot analysis (Fig. 1). Our analysis also produced recombinant protein of HECT-type E3 ligases without truncation and detected their ubiquitin-conjugation and polyubiquitination activity by luminescent analysis (Fig. 2C and 2D). The ubiquitin-conjugation of UPL5 was not observed when a reductant was added to the reaction (data not shown), suggesting that UPL5 formed a thioester bond with ubiquitin. In addition, the model RING-type E3 CIP8 possessed high polyubiquitin formation activity without substrate, consistent with what was reported previously [26]. Crude recombinant CIP8 formed polyubiquitin chains in the absence of exogenous E1 and E2 (Fig. 3C and 3D), suggesting that the wheat cell-free system might include enough endogenous E1 and E2 activity. It was reported that wheat germ extracts have only a partial ubiquitin pathway [30]. Although the process to isolate wheat germ extract is different from the conventional methods [33], this report strongly supports the existence of endogenous ubiquitin pathway in our wheat cell-free system. Indeed, luminescent analysis using crude recombinant protein showed slight polyubiquitin chain formation even in absence of recombinant E3 (Fig. 2D, Fig. 3C and Fig. 4A, "E3-" lane), indicating that wheat cell-free system might include not only E1 and E2, but E3s or other factors that accelerates the polyubiquitin chain formation. Further, quantitative immunoblot analysis using anti-ubiquitin antibody showed that free ubiquitin was also present in wheat germ extract at a concentration of at least 10 nM (data not shown). This is similar to the ubiquitin concentration supplied in the *in vitro* assay. Although we developed a convenient screening method to detect E3 activity in this study, removal of the endogenous ubiquitin and ubiquitin related components such as E1, E2 and E3, would yield a more sensitive assay. However, wheat cell-free system does not have 26S proteasome proteolytic activity (Fig. 5), indicating that using crude recombinant protein is sufficient for *in vitro* ubiquitination assays.

By using this method, we found that a previously uncharacterized RING type E3, At1g55530, possessed high polyubiquitination activity without exogenous E1 and E2 proteins (Fig. 4). This result suggested that the method developed here is expected to find the activity of other unknown E3 ligases such as At1g55530. Despite having only 32% sequence similarity, the E3s CIP8 and At1g55530 showed similar biochemical functions. Polyubiquitin chains formed by CIP8 and At1g55530 elongated on themselves, while another report showed that polyubiquitin chains were formed on E2 before transferring them to substrates [34]. This reflects that the pattern of polyubiquitin chain formation differs between individual E3s and that the detailed mechanisms are still unknown. These studies suggest the importance of functional analysis using active recombinant proteins. Although we developed a simple screen using crude recombinant E3s in absence of exogenous E1 and E2 (Fig. 4), this method could not detect the activity of some E3 ligases that were unable to utilize endogenous ubiquitination components in wheat cell-free system. The polyubiquitination activity of At5g20910 recombinant protein, expressed in *E. coli* in the presence of AtUBC8 [25], was not active in our *in vitro* system (Fig. 4A), suggesting that in some cases exogenous E2 and/or other components are necessary additions. Such modifications to the ubiquitination assays detailed here would help elucidate the biochemical features of E3s (e.g., addition of recombinant E2s to reaction mixture could give us further information about the E2–E3 specificity, and of other E3 components would lead to the elucidation of structure of complex type E3 ligase such as SCF).

Conclusion

In this study, we found that the wheat cell-free system was an excellent expression system to produce recombinant protein efficiently and to carry out *in vitro* ubiquitination assays without the interference of proteolytic activity. Coupled with luminescent analysis, detection of these ubiquitin reactions in the crude translation reaction mixture was possible. Thus, this method should be helpful for solving the complicated ubiquitin pathway in plant.

Methods

Construction of DNA Templates for Transcription

We used RAFL as templates. DNA templates of E2s and E3s for transcription were constructed by "Split-Primer"

PCR as described previously [17]. Primers used in this study are summarized in Additional file 1. The first round of PCR was performed on each cDNA template using 10 nM of each of the following primers: a target protein specific primer (5'-CCACCCACCACCACCAatgnnnnnnnnn nnnnnnnn-3'; lowercase indicates the 5'-coding region of the target gene) and the AODA2306 primer. Then, a second round of PCR was carried out to construct the templates for protein synthesis using a portion (5 μl) of the first PCR mix, 100 nM SPu primer, 100 nM AODA2303 primer and 1 nM deSP6E02 primer. GST tags were used according to the methods we described previously [17]. The transcription templates of two HECT-type E3 ligases, UPL7 and UPL5, were generated as C-terminal FLAG-tagged proteins using the Gateway System® (Invitrogen, Carlsbad, CA, USA). Briefly, the ORF sequences of UPL7 and UPL5 were amplified by PCR with sense and antisense primers containing attB1 and FLAG-attB2 sequences, respectively. According to the manufacturer's instructions (Invitrogen), these DNA fragments were subcloned into pDONR221 vector by BP reaction and then inserted into the Gateway-based pEU vector (pEU-E01-GW) by LR reaction. Using these recombinant vectors as templates, PCR was carried out with 100 nM SPu primer and 100 nM AODA2303 primer and used as transcription templates.

Cell-free Protein Synthesis

In vitro transcription and cell-free protein synthesis were performed as described [18]. Transcript was made from each of the DNA templates mentioned above using the SP6 RNA polymerase. The synthetic mRNAs were then precipitated with ethanol and collected by centrifugation using a Hitachi R10H rotor. Each mRNA (usually 30–35 μg) was washed and transferred into a translation mixture. The translation reaction was performed in the bilayer mode [35] with slight modifications. The translation mixture that formed the bottom layer consisted of 60 A260 units of the wheat germ extract (CellFree Sciences, Yokohama, Japan) and 2 μg creatine kinase (Roche Diagnostics K. K., Tokyo, Japan) in 25 μl of SUB-AMIX® (CellFree Sciences). The SUB-AMIX® contained (final concentrations) 30 mM Hepes/KOH at pH 8.0, 1.2 mM ATP, 0.25 mM GTP, 16 mM creatine phosphate, 4 mM DTT, 0.4 mM spermidine, 0.3 mM each of the 20 amino acids, 2.7 mM magnesium acetate, and 100 mM potassium acetate. SUB-AMIX® (125 μl) was placed on the top of the translation mixture, forming the upper layer. After incubation at 16°C for 15 h, the synthesized proteins were confirmed by SDS-PAGE. For biotin labeling, 1 μl of crude biotin ligase (BirA) produced by the wheat cell-free expression system was added to the bottom layer, and 0.5 μM (final concentration) of D-biotin (Nacalai Tesque, Inc., Kyoto, Japan) was added to both upper and bottom layers, as described previously [22].

Purification of E2 and E3 Proteins

Purification of GST-tagged protein was carried out according to the procedure described previously [36] with slight modification. Crude GST-tagged recombinant protein (450 μl) produced by the cell-free reaction was precipitated with glutathione sepharose™ 4B (GE Healthcare, Buckinghamshire, UK). The recombinant proteins were eluted with PBS buffer containing 0.1 U of AcTEV protease (Invitrogen) in order to cleave the GST tag from the protein.

Detection of Polyubiquitination by the Luminescent Method

In vitro polyubiquitination assays were carried out in a total volume of 15 μl consisting of 20 mM Tris-HCl pH 7.5, 0.2 mM DTT, 5 mM $MgCl_2$, (10 μM zinc acetate in the assays for RING-type E3s only), 3 mM ATP, 1 mg/ml BSA, 25 nM biotinylated ubiquitin, 25 nM FLAG-tagged ubiquitin, 1 μl of recombinant E2 (purified or crude) and 1 μl of recombinant E3 (purified or crude) in the presence or absence of 0.05 μM rabbit E1 (Boston Biochem, Cambridge, MA, USA) at 30°C for 1 hr in a 384-well Optiplate (PerkinElmer, Boston, MA, USA). In accordance with the AlphaScreen IgG (ProteinA) detection kit (Perkin Elmer) instruction manual, 10 μl of detection mixture containing 20 mM Tris-HCl pH 7.5, 0.2 mM DTT, 5 mM $MgCl_2$, 5 μg/ml Anti-FLAG antibody (Sigma-Aldrich, St. Louis, MO, USA), 1 mg/ml BSA, 0.1 μl streptavidin-coated donor beads and 0.1 μl anti-IgG acceptor beads were added to each well of the 384 Optiplate followed by incubation at 23°C for 1 hr. Luminescence was analyzed by the AlphaScreen detection program.

Detection of Ubiquitinated E2 by Immunoblot Analysis

Crude biotinylated recombinant E2 proteins (40 μl) were used for the ubiquitin-conjugating assay in a total reaction volume of 50 μl containing 20 mM Tris-HCl pH 7.5, 0.2 mM DTT, 5 mM $MgCl_2$, 3 mM ATP and 4 μM FLAG-tagged ubiquitin (Sigma) for 3 hr at 30°C. The reaction products were purified by Streptavidin Magnesphere Paramagnetics particles (Promega, Madison, WI, USA). After washing the beads with PBS buffer, recombinant E2s were boiled in 15 μl of SDS sample buffer containing 50 mM Tris-HCl pH 6.8, 2% SDS, 10% glycerol and 0.2% bromophenol blue, and then separated from the magnet beads. The proteins were separated by SDS-PAGE and transferred to PVDF membrane (Millipore Bedford, MA, USA) according to standard procedures. The blots were detected by the ECL plus detection system (GE Healthcare) with anti-FLAG antibody (Sigma) according to the manufacturer's procedure.

Detection of Polyubiquitination by the Immunoblot Analysis

For polyubiquitination of HECT-type E3 ligases, crude FLAG-tagged UPL recombinant protein (20 μl) was ubiq-

uitinated in a total reaction volume of 50 μl consisting of 20 mM Tris-HCl pH 7.5, 0.2 mM DTT, 5 mM $MgCl_2$, 3 mM ATP, 4 μM biotinylated ubiquitin and 20 μl of crude recombinant AtUBC8 for 3 hr at 30°C. Then, recombinant UPL protein was gathered by anti-FLAG M2 agarose (Sigma). After washing the agarose with PBS buffer, the recombinant UPL protein was boiled in 15 μl of SDS sample buffer and then separated from beads by centrifugation. For polyubiquitination of RING-type E3 ligases, the assay was carried out in 10 μl of reaction mixture containing 20 mM Tris-HCl pH 7.5, 0.2 mM DTT, 5 mM $MgCl_2$, 10 μM zinc acetate, 3 mM ATP, 1 mg/ml BSA, 4 μM FLAG- or His-tagged ubiquitin, 1 μl of purified or crude recombinant E2 and 1 μl of purified or crude recombinant E3 at 30°C for 3 hr. Then, 5 μl of three-fold concentrated SDS sample buffer was added to the reaction mixture and boiled for 5 min. Proteins were separated by SDS-PAGE and transferred to Hybond-LFP PVDF membrane (GE Healthcare) according to standard procedures. Immunoblot analysis was carried out with anti-FLAG antibody (Sigma) or anti-His antibody (GE Healthcare) according to the procedure described above. When detecting biotinylated ubiquitin, blots were treated with 5 μg/ml Alexa488-conjugated streptavidin (Invitrogen) in PBS buffer. After washing with PBS containing 0.1% Tween-20, the blot was analyzed by a Typhoon Imager (GE Healthcare) using the 532 nm laser and 526 emission filters.

Polyubiquitination Assay with 26S Proteasome Inhibitor

Polyubiquitination reaction was carried out as same procedure described above except addition of MG132 (Calbiochem, San Diego, CA, USA) at a final concentration of 20 μM to reaction mixture. Then, the protein on blot was detected by immunoblot analysis with anti-FLAG antibody or Alexa488-conjugated streptavidin.

Authors' contributions

HT conceived the study and performed the experiments, and contributed to writing the manuscript. MS and KS provided RAFL cDNA clones. AN conceived the study. YE conceived the study and supervised the work. TS conceived and designed the study, supervised the work and contributed to writing the manuscript.

Additional material

Additional file 1

AGI code of Arabidopsis genes and primer sequences used in this study.

AGI code of Arabidopsis genes and primer sequences used in this study. Click here for file [http://www.biomedcentral.com/content/supplementary/1471-2229-9-39-S1.xls]

Acknowledgements

This work was partially supported by the Special Coordination Funds for Promoting Science and Technology by the Ministry of Education, Culture, Sports, Science and Technology, Japan (T. S. and Y. E.). We thank Michael Andy Goren for proofreading this manuscript.

References

1. Bai C, Sen P, Hofmann K, Ma L, Goebl M, Harper JW, Elledge SJ: **SKP1 Connects Cell Cycle Regulators to the Ubiquitin Proteolysis Machinery through a Novel Motif, the F-Box.** *Cell* 1996, **86(2)**:263-274.
2. Chen Z, Hagler J, Palombella VJ, Melandri F, Scherer D, Ballard D, Maniatis T: **Signal-induced site-specific phosphorylation targets IκBα to the ubiquitin-proteasome pathway.** *Genes Dev* 1995, **9(13)**:1586-1597.
3. Pickart CM: **Mechanisms underlying ubiquitination.** *Annu Rev Biochem* 2001, **70**:503-533.
4. Smalle J, Vierstra RD: **The ubiquitin 26S proteasome proteolytic pathway.** *Annu Rev Plant Biol* 2004, **55**:555-590.
5. Borden KL: **RING domains: master builders of molecular scaffolds?** *J Mol Biol* 2000, **295(5)**:1103-1112.
6. Glickman MH, Ciechanover A: **The ubiquitin-proteasome proteolytic pathway: destruction for the sake of construction.** *Physiol Rev* 2002, **82(2)**:373-428.
7. Schnell JD, Hicke L: **Non-traditional functions of ubiquitin and ubiquitin-binding proteins.** *J Biol Chem* 2003, **278(38)**:35857-35860.
8. Hofmann RM, Pickart CM: **Noncanonical MMS2-encoded ubiquitin-conjugating enzyme functions in assembly of novel polyubiquitin chains for DNA repair.** *Cell* 1999, **96(5)**:645-653.
9. Yin XJ, Volk S, Ljung K, Mehlmer N, Dolezal K, Ditengou F, Hanano S, Davis SJ, Schmelzer E, Sandberg G, Teige M, Palme K, Pickart C, Bachmair A: **Ubiquitin lysine 63 chain forming ligases regulate apical dominance in Arabidopsis.** *Plant Cell* 2007, **19(6)**:1898-1911.
10. Hicke L: **A new ticket for entry into budding vesicles – ubiquitin.** *Cell* 2001, **106(5)**:527-530.
11. Vierstra RD: **The ubiquitin/26S proteasome pathway, the complex last chapter in the life of many plant proteins.** *Trends Plant Sci* 2003, **8(3)**:135-142.
12. Nelson DC, Lasswell J, Rogg LE, Cohen MA, Bartel B: **FKF1, a Clock-Controlled Gene that Regulates the Transition to Flowering in Arabidopsis.** *Cell* 2000, **101(3)**:331-340.
13. Osterlund MT, Hardtke CS, Wei N, Deng XW: **Targeted destabilization of HY5 during light-regulated development of Arabidopsis.** *Nature* 2000, **405(6785)**:462-466.
14. Stone SL, Williams LA, Farmer LM, Vierstra RD, Callis J: **KEEP ON GOING, a RING E3 ligase essential for Arabidopsis growth and development, is involved in abscisic acid signaling.** *Plant Cell* 2006, **18(12)**:3415-3428.
15. Rosebrock TR, Zeng L, Brady JJ, Abramovitch RB, Xiao F, Martin GB: **A bacterial E3 ubiquitin ligase targets a host protein kinase to disrupt plant immunity.** *Nature* 2007, **448(7151)**:370-374.
16. Kraft E, Stone SL, Ma L, Su N, Gao Y, Lau OS, Deng XW, Callis J: **Genome analysis and functional characterization of the E2 and RING-type E3 ligase ubiquitination enzymes of Arabidopsis.** *Plant Physiol* 2005, **139(4)**:1597-1611.
17. Sawasaki T, Ogasawara T, Morishita R, Endo Y: **A cell-free protein synthesis system for high-throughput proteomics.** *Proc Natl Acad Sci USA* 2002, **99(23)**:14652-14657.
18. Sawasaki T, Gouda MD, Kawasaki T, Tsuboi T, Tozawa Y, Takai K, Endo Y: **The wheat germ cell-free expression system: methods for high-throughput materialization of genetic information.** *Methods Mol Biol* 2005, **310**:131-144.
19. Kobayashi T, Kodani Y, Nozawa A, Endo Y, Sawasaki T: **DNA-binding profiling of human hormone nuclear receptors via fluorescence correlation spectroscopy in a cell-free system.** *FEBS Lett* 2008, **582(18)**:2737-2744.
20. Seki M, Narusaka M, Kamiya A, Ishida J, Satou M, Sakurai T, Nakajima M, Enju A, Akiyama K, Oono Y, Muramatsu M, Hayashizaki Y, Kawai J, Carninci P, Itoh M, Ishii Y, Arakawa T, Shibata K, Shinagawa A, Shinozaki K: **Functional annotation of a full-length Arabidopsis cDNA collection.** *Science* 2002, **296(5565)**:141-145.
21. Kus B, Gajadhar A, Stanger K, Cho R, Sun W, Rouleau N, Lee T, Chan D, Wolting C, Edwards A, Bosse R, Rotin D: **A high throughput**

screen to identify substrates for the ubiquitin ligase Rsp5. *J Biol Chem* 2005, **280(33)**:29470-29478.
22. Sawasaki T, Kamura N, Matsunaga S, Saeki M, Tsuchimochi M, Morishita R, Endo Y: **Arabidopsis HY5 protein functions as a DNA-binding tag for purification and functional immobilization of proteins on agarose/DNA microplate.** *FEBS Lett* 2008, **582(2)**:221-228.
23. Bates PW, Vierstra RD: **UPL1 and 2, two 405 kDa ubiquitin-protein ligases from Arabidopsis thaliana related to the HECT-domain protein family.** *Plant J* 1999, **20(2)**:183-195.
24. Downes BP, Stupar RM, Gingerich DJ, Vierstra RD: **The HECT ubiquitin-protein ligase (UPL) family in Arabidopsis: UPL3 has a specific role in trichome development.** *Plant J* 2003, **35(6)**:729-742.
25. Stone SL, Hauksdóttir H, Troy A, Herschleb J, Kraft E, Callis J: **Functional analysis of the RING-type ubiquitin ligase family of Arabidopsis.** *Plant Physiol* 2005, **137(1)**:13-30.
26. Hardtke CS, Okamoto H, Deng XW: **Biochemical evidence for ubiquitin ligase activity of the Arabidopsis COP1 interacting protein 8 (CIP8).** *Plant J* 2002, **30(4)**:385-394.
27. Yamauchi K, Wada K, Tanji K, Tanaka M, Kamitani T: **Ubiquitination of E3 ubiquitin ligase TRIMa and its potential role.** *FEBS J* 2008, **275(7)**:1540-1555.
28. Waxman L, Fagan JM, Goldberg AL: **Demonstration of two distinct high molecular weight proteases in rabbit reticulocytes, one of which degrades ubiquitin conjugates.** *J Biol Chem* 1987, **262(6)**:2451-2457.
29. Chen ZJ, Parent L, Maniatis T: **Site-Specific Phosphorylation of IκBα by a Novel Ubiquitination-Dependent Protein Kinase Activity.** *Cell* 1996, **84(6)**:853-862.
30. Hatfield PM, Vierstra RD: **Ubiquitin-dependent proteolytic pathway in wheatgerm: Isolation of multiple forms of ubiquitin-activating enzyme, E1.** *Biochemistry* 1989, **28**:735-742.
31. Wu CJ, Conze DB, Li T, Srinivasula SM, Ashwell JD: **Sensing of Lys 63-linked polyubiquitination by NEMO is a key event in NF-κB activation.** *Nature Cell Biol* 2006, **8(4)**:398-406.
32. Yin XJ, Volk S, Ljung K, Mehlmer N, Dolezal K, Ditengou F, Hanano S, Davis SJ, Schmelzer E, Sandberg G, Teige M, Palme K, Pickart C, Bachmaira A: **Ubiquitin lysine 63 chain-forming ligases regulate apical dominance in Arabidopsis.** *Plant Cell* 2007, **19(6)**:1898-1911.
33. Madin K, Sawasaki T, Ogasawara T, Endo Y: **A highly efficient and robust cell-free protein synthesis system prepared from wheat embryos: Plants apparently contain a suicide system directed at ribosomes.** *Proc Natl Acad Sci USA* 2000, **97(2)**:559-564.
34. Li W, Tu D, Brunger AT, Ye Y: **A ubiquitin ligase transfers preformed polyubiquitin chains from a conjugating enzyme to a substrate.** *Nature* 2007, **446(7133)**:333-337.
35. Sawasaki T, Hasegawa Y, Tsuchimochi M, Kamura N, Ogasawara T, Kuroita T, Endo Y: **A bilayer cell-free protein synthesis system for high-throughput screening of gene products.** *FEBS Lett* 2002, **514(1)**:102-105.
36. Masaoka T, Nishi M, Ryo A, Endo Y, Sawasaki T: **The wheat germ cell-free based screening of protein substrates of calcium/calmodulin-dependent protein kinase II delta.** *FEBS Lett* 2008, **582(13)**:1795-1801.

THE JOURNAL OF BIOLOGICAL CHEMISTRY VOL. 285, NO. 3, pp. 1754–1764, January 15, 2010

Pin1 Promotes Transforming Growth Factor-β-induced Migration and Invasion*

Received for publication, September 8, 2009, and in revised form, November 16, 2009 Published, JBC Papers in Press, November 17, 2009, DOI 10.1074/jbc.M109.063826

Isao Matsuura[‡§¶‖1], Keng-Nan Chiang[‖], Chen-Yu Lai[‖], Dongming He[‡§¶], Guannan Wang[‡§¶], Romila Ramkumar[‡§¶], Takafumi Uchida[**], Akihide Ryo[‡‡], Kunping Lu[§§], and Fang Liu[‡§¶2]

From the [‡]Center for Advanced Biotechnology and Medicine and [§]Susan Lehman Cullman Laboratory for Cancer Research, Department of Chemical Biology, Ernest Mario School of Pharmacy, Rutgers, The State University of New Jersey and the [¶]Cancer Institute of New Jersey, Piscataway, New Jersey 08854, [‖]Division of Molecular Genomics and Medicine, National Health Research Institutes, Zhunan Town, Miaoli County 350, Taiwan, [**]Molecular Enzymology, Graduate School of Agricultural Science, Tohoku University, Miyagi 981-8555, Japan, [‡‡]Department of Microbiology, Yokohama City University School of Medicine, Yokohama 236-0004, Japan, and [§§]Cancer Biology Program, Division of Hematology/Oncology, Department of Medicine, Beth Israel Deaconess Medical Center, Harvard Medical School, Boston, Massachusetts 02105

Transforming growth factor-β (TGF-β) regulates a wide variety of biological activities. It induces potent growth-inhibitory responses in normal cells but promotes migration and invasion of cancer cells. Smads mediate the TGF-β responses. TGF-β binding to the cell surface receptors leads to the phosphorylation of Smad2/3 in their C terminus as well as in the proline-rich linker region. The serine/threonine phosphorylation sites in the linker region are followed by the proline residue. Pin1, a peptidyl-prolyl cis/trans isomerase, recognizes phosphorylated serine/threonine-proline motifs. Here we show that Smad2/3 interacts with Pin1 in a TGF-β-dependent manner. We further show that the phosphorylated threonine 179-proline motif in the Smad3 linker region is the major binding site for Pin1. Although epidermal growth factor also induces phosphorylation of threonine 179 and other residues in the Smad3 linker region the same as TGF-β, Pin1 is unable to bind to the epidermal growth factor-stimulated Smad3. Further analysis suggests that phosphorylation of Smad3 in the C terminus is necessary for the interaction with Pin1. Depletion of Pin1 by small hairpin RNA does not significantly affect TGF-β-induced growth-inhibitory responses and a number of TGF-β/Smad target genes analyzed. In contrast, knockdown of Pin1 in human PC3 prostate cancer cells strongly inhibited TGF-β-mediated migration and invasion. Accordingly, TGF-β induction of *N*-cadherin, which plays an important role in migration and invasion, is markedly reduced when Pin1 is depleted in PC3 cells. Because Pin1 is overexpressed in many cancers, our findings highlight the importance of Pin1 in TGF-β-induced migration and invasion of cancer cells.

Transforming growth factor-β (TGF-β)[3] is a multifunctional cytokine that controls various fundamental biological activities such as cell proliferation, differentiation, migration, adhesion, and apoptosis (1). Disruption of the TGF-β signaling pathways is associated with a number of human diseases, especially cancer (2–8). TGF-β has two opposite roles in cancer. It is a potent tumor suppressor during the early stages of tumorigenesis through its growth-inhibitory effects and apoptosis-promoting function (2–8). TGF-β promotes cancer progression and metastasis at later stages (2–8).

TGF-β signal transduction is mediated by two types of cell surface serine/threonine kinase receptors (TβRI and TβRII) and downstream effectors, the Smad family proteins (9–14). TGF-β binding induces the formation and activation of a receptor complex containing TβRI and TβRII. The activated TβRI directly phosphorylates Smad2 and Smad3 at the SS*X*S motif in their C-tails. The phosphorylated Smad2 and Smad3 then form a complex with Smad4 and together accumulate in the nucleus to regulate transcription of a wide variety of target genes, leading to distinct biological effects in a cell context-dependent manner (9–14).

In addition to the C-tail phosphorylation sites for the receptor kinase, Smad2 and Smad3 contain multiple serine/threonine phosphorylation sites in the proline-rich linker region that connects the N- and C-terminal domains. Among them, several phosphorylation sites are followed by the proline residue and can be phosphorylated by proline-directed kinases, such as the mitogen-activated protein kinase superfamily members that include ERK, c-Jun N-terminal kinase, and p38, the cyclin-dependent kinase family members, and glycogen synthase kinase-3 (11, 15–38).

We and others have recently shown that three sites Thr-179, Ser-204, and Ser-208 in the Smad3 linker region are phosphorylated in response to TGF-β (30, 36–38) and that the cy-

* This work was supported by National Institutes of Health Grant CA93771 (to F. L.). This work was also supported by the National Health Research Institutes (to I. M.).

[1] To whom correspondence may be addressed: Division of Molecular Genomics and Medicine, National Health Research Institutes, No. 35 Keyan Rd., Zhunan Town, Miaoli County 350, Taiwan. Tel.: 886-37-246-166 (ext. 35369); Fax: 886-37-586-459; E-mail: imatsuura@nhri.org.tw.

[2] To whom correspondence may be addressed: Center for Advanced Biotechnology and Medicine, Rutgers University, 679 Hoes Lane, Piscataway, NJ 08854. Tel.: 732-235-5372; Fax: 732-235-4850; E-mail: fangliu@cabm.rutgers.edu.

[3] The abbreviations used are: TGF-β, transforming growth factor-β; TβRI, TGF-β type I receptor; TβRII, TGF-β type II receptor; EGF, epidermal growth factor; ERK, extracellular-signal regulated kinase; Smurf2, Smad ubiquitination regulatory factor 2; Pin1, protein interacting with NIMA (never in mitosis A); shRNA, small hairpin RNA; GST, glutathione *S*-transferase; GAPDH, glyceraldehydes-3-phosphate dehydrogenase; FBS, fetal bovine serum; EPSM, Erk/proline-directed kinase site mutant.

clin-dependent kinase family members and glycogen synthase kinase-3 are responsible for the phosphorylation (36–38). The Thr-179 and Ser-208 are phosphorylated by the cyclin-dependent kinase family members in response to TGF-β (36), whereas the Ser-204 is phosphorylated by glycogen synthase kinase-3 in response to TGF-β (36, 37). We have further shown that the C-tail phosphorylation is necessary for the linker phosphorylation in response to TGF-β (36). When the C-tail phosphorylation sites in Smad3 are mutated, the linker sites are not phosphorylated in response to TGF-β (36).

Interestingly, these three same sites, Thr-179, Ser-204, and Ser-208, in the Smad3 linker region are also phosphorylated by ERK in response to EGF treatment and Ser-208 is the best ERK phosphorylation site in Smad3 (29). The ERK phosphorylation does not require the C-tail phosphorylation. When the C-tail phosphorylation sites in Smad3 are mutated, ERK still phosphorylates these three sites in response to EGF treatment (36).

The Smad2 linker region is also phosphorylated in response to TGF-β or EGF (11, 15–17, 19–25, 30, 31, 36). However, due to the lack of specific phosphopeptide antibodies against each of the putative phosphorylation sites and the lack of mapping of the phosphorylation sites by other methods, the exact sites in the Smad2 linker region that are phosphorylated in response to TGF-β or EGF remain to be determined.

Pin1 is a peptidyl-prolyl cis/trans isomerase that recognizes the phosphorylated serine/threonine-proline motifs in certain proteins and catalyzes prolyl cis/trans isomerization (39–41). The prolyl isomerization induces conformational changes, leading to distinct effects in different target proteins, such as increased stability, increased turnover, alteration of the sensitivity to phosphatases, alteration in subcellular localizations, and altered enzymatic activities, and enabling protein-protein interactions (39–41). Since its discovery, a number of Pin1 targets have been identified, indicating the importance of Pin1 in the cellular physiology (39–41). The various studies also suggest that the effects of Pin1 are cell context-dependent (39–41). Pin1 is overexpressed in many cancers, such as in prostate, breast, lung, colon, and hepatocellular carcinoma (39–51). In prostate cancer, overexpression of PIN1 is correlated with a higher probability of tumor recurrence and a shorter period to tumor recurrence after radical prostatectomy (52). In addition to cancer, Pin1 is also linked with other diseases, such as Alzheimer disease and asthma (39, 41).

Because the Thr-179, Ser-204, and Ser-208 phosphorylation sites in Smad3 are followed by the proline residue, they constitute putative Pin1 binding sites. It is possible that certain or all of these sites serve as the Pin1-binding site(s) when they are phosphorylated. Recently, Nakano *et al.* (53) reported that Pin1 can associate with Smad2 and Smad3 to enhance their interaction with Smurf2 (Smad ubiquitination regulatory factor 2), a HECT domain E3 ubiquitin ligase, resulting in enhanced Smad ubiquitination and reduced Smad2/3 levels. We show in this report that Pin1 binds to Smad2/3 in a TGF-β-dependent manner and that the phosphorylated Thr-179-proline is the major binding site for Pin1 in Smad3 in response to TGF-β. We further show that knockdown of Pin1 does not have a significant effect on TGF-β-induced growth-inhibitory response, as analyzed in the human HaCaT keratinocytes. On the contrary, knockdown of Pin1 in human PC3 prostate cancer cells significantly inhibited TGF-β-induced cell migration and invasion. Our study uncovered an important role of Pin1 in TGF-β-mediated cancer cell migration and invasion.

EXPERIMENTAL PROCEDURES

Constructs, Antibodies, and Chemical Inhibitors—Mammalian expression plasmids for Smad3, its phosphorylation mutants, and TβRI were described previously (26, 36). Plasmids for GST-Pin1, pSUPER-puro-shRNA against Pin1 or the scrambled control were also described previously (54, 55). The Smad3-specific peptide antibody and the Smad2-specific peptide antibody were from Invitrogen. The Smad2/3 antibody that was raised against the full-length Smad3 and recognizes both Smad2 and Smad3, the Pin1 polyclonal antibody, the SIP1 polyclonal antibody, and the actin antibody was purchased from Santa Cruz Biotechnology, Inc. The N-cadherin antibody was purchased from Upstate Biotechnology. The Slug monoclonal antibody (clone 2B6) was obtained from the Millipore Corp. The Snail polyclonal antibody was from ABGENT. The E-cadherin monoclonal antibody (clone 67A4) was from Chemicon International. Smad3 phospho-specific antibodies were described previously (26, 36). The Smad3 (C-tail) phosphopeptide antibody was generously provided by Dr. Edward B. Leof (Mayo Clinic Cancer Center, Rochester, MN). Horseradish peroxidase-conjugated secondary antibodies were obtained from Pierce or Chemicon International. ECL Western blot reagents were purchased from Roche Applied Science or Millipore Corp. PiB, diethyl-1,3,6,8-tetrahydro-1,3,6,8-tetraoxobenzo[lmn][3,8]phenan throline-2,7-diacetate, a Pin1 inhibitor, was purchased from Merck.

Cell Culture, Transfection, and Retroviral Infection—Human PC3 prostate cancer cell line was cultured in RPMI1640 with 10% fetal bovine serum (FBS), 1% penicillin/streptomycin. Amphotropic Phoenix cells (Phoenix A) were grown in Dulbecco's modified Eagle's medium with 10% FBS, 1% penicillin/streptomycin. Human HaCaT keratinocytes and human HEK293T cells were cultured in minimum essential medium, 10% FBS, 1% penicillin/streptomycin. L17, a TβRI-deficient cell line derived from the Mv1Lu mink lung epithelial cell line, was maintained in minimum essential medium without histidine but plus histidinol, 10% FBS, 1% penicillin/streptomycin. The L17 cells and the 293T cells were transfected by DEAE-dextran and Lipofectamine Plus reagent (Invitrogen), respectively, as previously described (26, 36). For shRNA retrovirus production, Phoenix A cells were transfected with pSUPER-puro-shRNA targeting Pin1 or a scrambled control by Lipofectamine Plus reagent. HaCaT and PC3 cells were infected several times with the retrovirus targeting Pin1 or the scrambled control. The infected cells were selected with 5 μg/ml puromycin.

GST Pulldown Assay and Coimmunoprecipitation Assay—GST and GST-Pin1 were expressed in bacteria strain BL21 (DE3). GSH-Sepharose beads containing GST or GST-Pin1 were prepared as described previously (26). For analysis of Smad interaction with GST-Pin1, HaCaT cells were serum-starved before the addition of EGF or TGF-β. Cells were then treated with either 50 ng/ml EGF for 15 min or 300 pM TGF-β for 1 h for maximal induction of Smad3 phosphorylation in the linker sites. Cells were lysed with the lysis buffer (10 mM Tris-

Cl, pH 7.8, 150 mM NaCl, 1% Nonidet P-40, 1 mM EDTA, 1× complete protease inhibitor mixture (Roche Applied Science), 1 mM phenylmethylsulfonyl fluoride, 25 mM NaF, 10 mM sodium pyrophosphate, 10 mM β-glycerophosphate, 1 mM dithiothreitol, 1 μg/ml RNase A). Cell lysates (300 μg) were incubated with 10 μl of either GST or GST-Pin1 beads at 4 °C for 2 h. The beads were washed with the cell lysis buffer 5 times, and the bound proteins on the beads were eluted by SDS sample buffer. For analysis of Smad3 and its mutants for interaction with GST-Pin1, L17 cells were cotransfected with expression plasmids for wild type or a mutant Smad3 together with TβRI, and the cells were treated with or without TGF-β for 1 h. Alternatively, the HEK293T cells were transfected with the wild type Smad3 or a mutant Smad3 and treated with TGF-β for 1 h. The cell lysates were subjected to GST pulldown assays as described above.

For coimmunoprecipitation assays to detect Smad2/3 and Pin1 interaction at endogenous levels, HaCaT cells were treated with or without TGF-β for 1 h, and the cell lysates (800 μg) were precleared by incubation with 20 μl of protein A/G beads at 4 °C for 0.5 h. The precleared lysates were then incubated with 2.5 μg of either control IgG or the Smad2/3 antibody at 4 °C overnight. Protein A/G-beads were then added and incubated for 2 h. The beads were washed 5 times with the lysis buffer and eluted with SDS sample buffer. Proteins eluted from the beads were subjected to Western blot analysis using the polyclonal Pin1 antibody by fresh ECL reagents (Roche Applied Science).

Thymidine Incorporation Assay—[^{3}H]Thymidine incorporation assay was performed as described previously (26). In brief, 2×10^5 shRNA-transduced HaCaT cells were seeded on 6-well plates in triplicate for 24 h and then treated with or without TGF-β at various concentrations for 24 h. 5 μCi of [^{3}H]thymidine was added to each well during the last 4 h of the incubation. Cells were then washed 3 times with phosphate-buffered saline, fixed with 95% methanol, and extracted with 0.2 N NaOH. The extracts were counted for radioactivity. The results represent the average and S.D. of three independent experiments.

RNA Preparation and Northern Blot Analysis—shRNA-transduced HaCaT cells were treated with or without 300 pM TGF-β for 8 h. Poly(A)$^+$ RNA was prepared by the FAST track kit (Invitrogen). Northern blot was performed as previously described (56). Briefly, poly(A)$^+$ RNA was separated on a 1% formaldehyde-agarose gel, transferred to a nylon membrane, and hybridized with a random primed ^{32}P-labeled probe. The following probes were used: Pin1, p15, p21, Smad7, JunB, PAI-1, Bcl-2, Bub-1, and glyceraldehydes-3-phosphate dehydrogenase (GAPDH).

Cell Migration and Invasion Assays—Cell migration and invasion assays were performed essentially as previously described (57, 58). shRNA-transduced PC3 cells were serum-starved (0.2% FBS) overnight and then treated with or without 500 pM TGF-β for 48 h. The cells were trypsinized and resuspended in RPM1640, 0.1% bovine serum albumin at 3.3×10^5 cells/ml for migration assay and at 6.6×10^5 cells/ml for invasion assay. 300 μl of the suspension was applied onto a Millicell Hanging Cell Culture Insert (8 μm pore size, Millipore) in 24-well plates with the media containing 10% FBS at the bottom. For the invasion assay, the insert was precoated with Matrigel (BD Biosciences, 1:4 diluted with RPM1640, 0.1% bovine serum albumin). TGF-β (500 pM) was included in the medium for those cells that had been treated with TGF-β. The cells were incubated at 37 °C for 15 h for migration assay or 24 h for invasion assay. Medium was removed from the insert, and the upper side of the membranes was wiped with a cotton swab to remove un-migrated cells. Migrated cells at the bottom of the insert were stained with 0.1% crystal violet, 20% ethanol, and 1% formaldehyde. The number of migrated cells was counted for quantification. The results represent the average and S.D. of four independent experiments.

RESULTS

Pin1 Binds to Smad2/3 Specifically in a TGF-β-dependent Manner—We previously showed that phosphorylation of three serine/threonine residues (Thr-179, Ser-204, and Ser-208) in the proline-rich linker region of Smad3 is induced by both EGF and TGF-β (29, 36). These phosphorylation sites are followed by the proline residue, thus constituting putative Pin1 binding sites. We therefore examined the possibility of whether Smad3 binds to Pin1 in response to EGF or TGF-β. We treated human HaCaT keratinocytes with either EGF or TGF-β. The cell lysates were then subjected to GST pulldown assays with GST-Pin1 beads or the control GST beads followed by immunoblot with an antibody against Smad3. As shown in Fig. 1*A*, Pin1 binds specifically to the TGF-β-stimulated Smad3. To confirm this result, we analyzed the precipitates by immunoblot with phospho-specific antibodies against Thr-179, Ser-204, and Ser-208 in Smad3. Although the phosphorylation of Thr-179, Ser-204, and Ser-208 in Smad3 was induced to a similar extent by EGF and TGF-β (Fig. 1*A*), the phosphorylated Thr-179, Ser-204, and Ser-208 were detected in GST-Pin1 beads only in response to TGF-β treatment (Fig. 1*A*). Very little of Thr(P)-179, Ser(P)-204, or Ser(P)-208 was detected in the GST-Pin1 beads in response to EGF treatment (Fig. 1*A*).

Because the linker region of Smad2 is also phosphorylated in response to EGF or TGF-β (11, 15–17, 19–25, 30, 31, 36), we analyzed whether Pin1 binds to Smad2 after EGF or TGF-β treatment. HaCaT cells were treated with EGF or TGF-β. The cell lysates were incubated with GST-Pin1 beads or the GST control beads. The precipitates were then analyzed by immunoblots with an antibody against Smad2. As shown in Fig. 1*B*, Pin1 binds to Smad2 in response to TGF-β but not in response to EGF.

To provide further evidence that Smad2/3 binds to Pin1 in response to TGF-β, we analyzed whether Smad2/3 interacts with Pin1 after TGF-β treatment at endogenous levels. HaCaT cells were treated with or without TGF-β. Cell lysates were then immunoprecipitated with a Smad2/3 antibody that was raised against the full-length Smad3 and recognizes both Smad3 and Smad2. The immunoprecipitates were then analyzed by immunoblot with a Pin1-specific antibody. As shown in Fig. 1*C*, Pin1 binds to Smad2/3 in response to TGF-β at endogenous levels.

Pin1 Binding Requires Smad3 Phosphorylation in the C-tail and at the Thr-179 Site in the Linker Region—As described above, although EGF and TGF-β induces the phosphorylation of the same sites in the Smad3 linker region, Pin1 binds only to TGF-β-induced Smad3. We reasoned that there should be

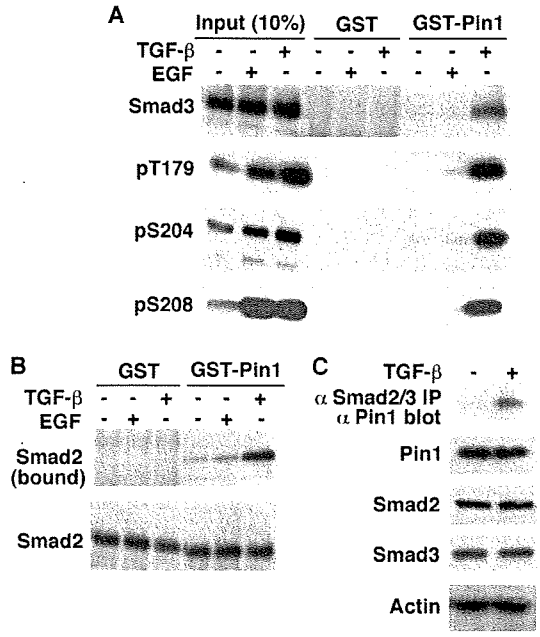

FIGURE 1. **Pin1 binds to Smad2/3 in a TGF-β-dependent manner.** *A*, TGF-β, but not EGF, induces Pin1-Smad3 interaction. HaCaT cells were treated with 300 pM TGF-β for 1 h or with 50 ng/ml EGF for 15 min for maximal induction of Smad3 phosphorylation in the linker region. The cell lysates were incubated with either GST or GST-Pin1 beads. The bound proteins were analyzed by immunoblot with an antibody against Smad3. The bound proteins were also analyzed by immunoblot with specific phosphopeptide antibodies against the phosphorylated Thr-179, Ser-204, and Ser-208 in the Smad3 linker region. *B*, TGF-β, but not EGF, induces Pin1-Smad2 interaction. HaCaT cells were treated with TGF-β or EGF as described in *A*. The cell lysates were incubated with GST or GST-Pin1 beads. The bound proteins were analyzed by immunoblot with an antibody against Smad2. The Smad2 levels in the cell lysates were also analyzed as a control. *C*, TGF-β induces Pin1-Smad2/3 interactions at endogenous protein levels. HaCaT cells were treated with or without TGF-β for 1 h. The cell lysates were immunoprecipitated with an antibody that was raised against the full-length Smad3 and recognizes both Smad3 and Smad2. The precipitates were analyzed by immunoblot with an antibody against Pin1. The expression levels of Pin1, Smad2, Smad3, and actin in the cell lysates were also analyzed as controls.

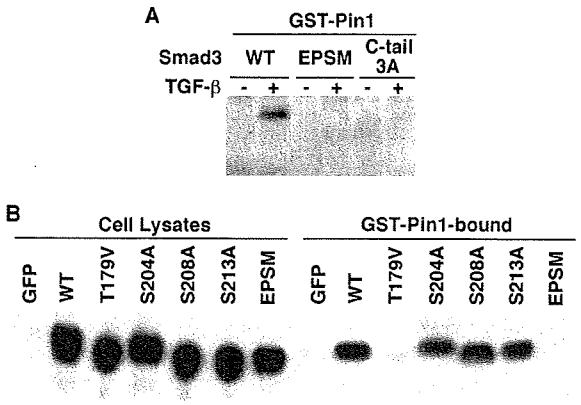

FIGURE 2. **Pin1 binding to Smad3 requires both the linker and the C-tail phosphorylation, and the Thr-179 is the major binding site for Pin1.** *A*, phosphorylation of both the linker and the C-tail in Smad3 is necessary for interaction with Pin1 in response to TGF-β. L17 cells were cotransfected with TβRI along with the wild type (*WT*) Smad3, a linker phosphorylation mutant (*EPSM*), or a C-tail phosphorylation mutant (*C-tail 3A*). Cells were then treated with or without 300 pM TGF-β for 1 h. The cell lysates were incubated with GST-Pin1 beads. The bound proteins were analyzed by immunoblot with the Smad3 antibody. *B*, Thr-179 is the major binding site in Smad3 for interaction with Pin1 in response to TGF-β. HEK293T cells were transfected with the wild type Smad3, a linker phosphorylation mutant Smad3, or a control plasmid that encodes GFP. Cells were treated with 300 pM TGF-β for 1 h. The cell lysates were incubated with the GST-Pin1 beads. The bound proteins were analyzed by immunoblot with the Smad3 antibody. The expression levels of the various Smad3 proteins were also analyzed as a control.

other components in Smad3 that contributes to this specificity. In addition to the linker sites, TGF-β induces phosphorylation of the C-tail of Smad3. Because this phosphorylation was absent in EGF-stimulated Smad3, we tested whether mutation of the C-tail phosphorylation sites had any effect on TGF-β-dependent Smad3-Pin1 interaction. We transfected the L17 cells with TβRI along with the wild type Smad3, its linker region Erk/proline-directed kinase site mutant (EPSM) that contained mutations at the four putative Pin1 sites, or the C-tail phosphorylation site mutant (C-tail 3A). As shown in Fig. 2*A*, upon TGF-β treatment, Smad3 formed a complex with Pin1. Consistent with the idea that the Pin1-binding site(s) is located in the linker region, the EPSM mutant was unable to bind to Pin1 (Fig. 2*A*). Interestingly, the C-tail 3A mutant also abolished the Pin1 binding (Fig. 2*A*), although it still contains the intact Pin1-binding site(s) in the linker region. Our previous study has shown that when the Smad3 C-tail is mutated, the TGF-β-induced linker phosphorylation is abolished but has no effect on EGF-induced linker phosphorylation (36), suggesting that the C-tail phosphorylation is necessary for the linker phosphorylation in response to TGF-β. Thus, abrogation of Pin1 binding by the C-tail 3A mutant suggests that the C-tail phosphorylation by the receptor kinase is necessary for Smad3 binding to Pin1. Although EGF and TGF-β induce phosphorylation at the same linker sites, the structure of Smad3 at the C termini is different under the two conditions. Pin1 binding may require a discrete C termini structure, which results from phosphorylation of the *SXS* motif (10). Taken together, our result suggests that Pin1 binding requires the phosphorylation of both the C-tail and the linker.

In the Smad3 linker region there are four putative Pin1 binding sites. These include the Thr-179, Ser-204, and Ser-208. In addition, it includes the Ser-213 site, which is phosphorylated by cyclin-dependent kinase at the basal state (26). We mutated these four sites individually. GST pulldown assays with these mutants revealed that Thr-179 → Val mutation (T179V) dramatically reduced Pin1 binding in response to TGF-β. In contrast, mutation of any of the other three sites had little effects (Fig. 2*B*). As a control, the EPSM mutant was unable to bind to the Pin1 (Fig. 2*B*). Thus, we conclude that Thr-179 is the major Pin1-binding site in Smad3.

Depletion of Pin1 Does Not Have a Significant Effect on the Smad2/3 Levels, on TGF-β-induced Smad3 Linker Phosphorylation, or on TGF-β-induced Smad2/3 Nuclear Accumulation—To determine the consequence of Pin1 binding in TGF-β signaling, we generated stable cell lines in HaCaT cells that knock down the expression of Pin1 or a scrambled control. As shown in Fig. 3*A*, Pin1 is very effectively depleted by shRNA against Pin1. The depletion of Pin1 has little effect on Smad2 or Smad3 levels in HaCaT cells (Fig. 3*A*).

Because Pin1 binding to Smad3 may regulate TGF-β signaling by affecting the phosphorylation levels at Thr-179 and potentially also at the Ser-204 and Ser-208 sites, we analyzed

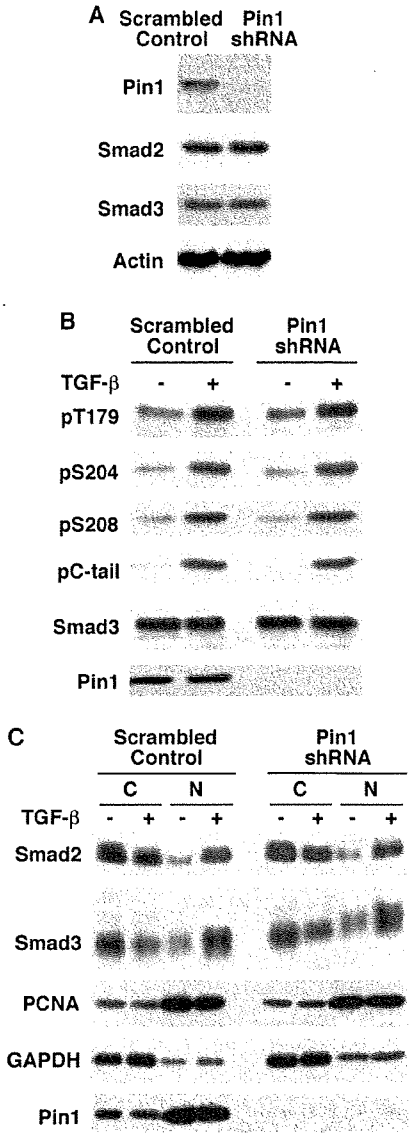

FIGURE 3. **Knockdown of Pin1 does not have a significant effect on Smad2/3 levels, on TGF-β-induced linker and C-tail phosphorylation of Smad3, or on TGF-β-induced Smad2/3 nuclear accumulation.** *A*, depletion of Pin1 has little effect on Smad2/3 levels in HaCaT cells. Stable HaCaT cell lines with an shRNA targeting Pin1 or the scrambled control were generated. The cell lysates were analyzed by immunoblot for Pin1, Smad2, and Smad3 levels. Actin levels were also analyzed as a control. *B*, depletion of Pin1 does not have a significant effect on TGF-β-induced linker and C-tail phosphorylation of Smad3 in HaCaT cells. The Pin1 knockdown HaCaT cells and the scrambled control HaCaT cells were treated with or without TGF-β for 1 h. The cell lysates were analyzed by immunoblot with phosphopeptide antibodies against the phosphorylated Thr-179, Ser-204, Ser-208, and the C-tail. Smad3 and Pin1 expression levels were also analyzed as controls. *C*, depletion of Pin1 does not affect TGF-β-induced Smad2/3 nuclear accumulation in HaCaT cells. The Pin1 knockdown HaCaT cells and the scrambled control HaCaT cells were treated with or without TGF-β for 1 h. Cells were then harvested and fractionated into the cytoplasmic (*C*) and nuclear (*N*) fractions. The same amount of proteins from the cytoplasmic fraction and nuclear fraction was analyzed for Smad2, Smad3, and Pin1 levels by immunoblot. GAPDH and proliferating cell nuclear antigen (*PCNA*) serve as cytoplasmic and nuclear markers, respectively.

whether Pin1 knockdown affected the phosphorylation levels of Thr-179, Ser-204, or Ser-208 in response to TGF-β. As shown in Fig. 3*B*, depletion of Pin1 did not have a significant effect on the TGF-β-induced phosphorylation levels at these three sites or a significant effect on the Smad3 C-tail phosphorylation in response to TGF-β (Fig. 3*B*).

We also analyzed whether depletion of Pin1 affects TGF-β-induced nuclear accumulation of Smad2 and Smad3. The Pin1 knockdown HaCaT cells and the scrambled control HaCaT cells were treated with or without TGF-β for 1 h. Cells were then harvested and fractionated into the cytoplasmic and nuclear fractions. As shown in Fig. 3*C*, knockdown of Pin1 does not affect Smad2 or Smad3 nuclear accumulation in response to TGF-β. Pin1 is predominantly localized in the nucleus as previously reported (59), and its subcellular localization was not affected by TGF-β treatment (Fig. 3*C*). The GAPDH serves as a marker for cytoplasmic localization, whereas the proliferating cell nuclear antigen serves as a marker for nuclear localization.

Depletion of Pin1 Does Not Have a Significant Effect on TGF-β-induced Growth-inhibitory Effects—One of the major functions of the TGF-β/Smad pathway is to induce growth inhibition. We therefore analyzed whether Pin1 knockdown affected TGF-β/Smad-mediated growth inhibition in HaCaT cells, which are strongly inhibited by TGF-β. The Pin1 knockdown HaCaT cells and the scrambled control HaCaT cells were treated with or without TGF-β at various doses and then subjected to [^{3}H]thymidine incorporation assay. As shown in Fig. 4*A*, the scrambled control HaCaT cells are highly sensitive to TGF-β, and the Pin1 knockdown HaCaT cells are overall similar to the scrambled control in terms of TGF-β sensitivity. At 5 pM TGF-β, the Pin1 knockdown cells are a little more sensitive to TGF-β than the control cells (Fig. 4*A*). At a higher concentration of TGF-β, the control HaCaT cells are slightly more sensitive to TGF-β (Fig. 4*A*). Although we don't understand why there is a subtle difference in TGF-β sensitivity at different concentrations between the control cells and the Pin1 knockdown cells, the results clearly indicate that knockdown of Pin1 does not have a significant effect on TGF-β-induced growth inhibition.

Previous studies have shown that TGF-β/Smad-mediated growth inhibition resulted from changes in the expression of cell cycle-related genes, such as induction of the expression of the cyclin-dependent kinase inhibitors p15 and p21 (2, 14, 60–65). We therefore analyzed whether knockdown of Pin1 affected several TGF-β/Smad target genes. The control HaCaT cells and the Pin1 knockdown HaCaT cells were treated with or without TGF-β. Poly(A)$^+$ RNA were isolated from the cells and then subjected to Northern blot analysis. As a control, the Northern blot confirmed that Pin1 expression was essentially abolished in the knockdown cells (Fig. 4*B*). Consistent with the [^{3}H]thymidine incorporation assay above, TGF-β induction of p15 and p21 was similar between the control cells and the Pin1 knockdown cells (Fig. 4, *B* and *C*). We also analyzed several other TGF-β/Smad target genes, including Smad7, JunB, and PAI-1 (2, 14, 56, 66–69). As shown in Fig. 4, *B* and *C*, TGF-β induction of Smad7, JunB, and PAI-1 was overall similar between the control cells and the Pin1 knockdown cells. For JunB, the basal levels and TGF-β-induced levels are modestly higher in Pin1 knockdown cells than in control cells. For PAI-1, the basal levels and TGF-β-induced levels are slightly higher in the control cells than in the Pin1 knockdown cells. We also analyzed the expression of Bcl2, which is reduced in response to

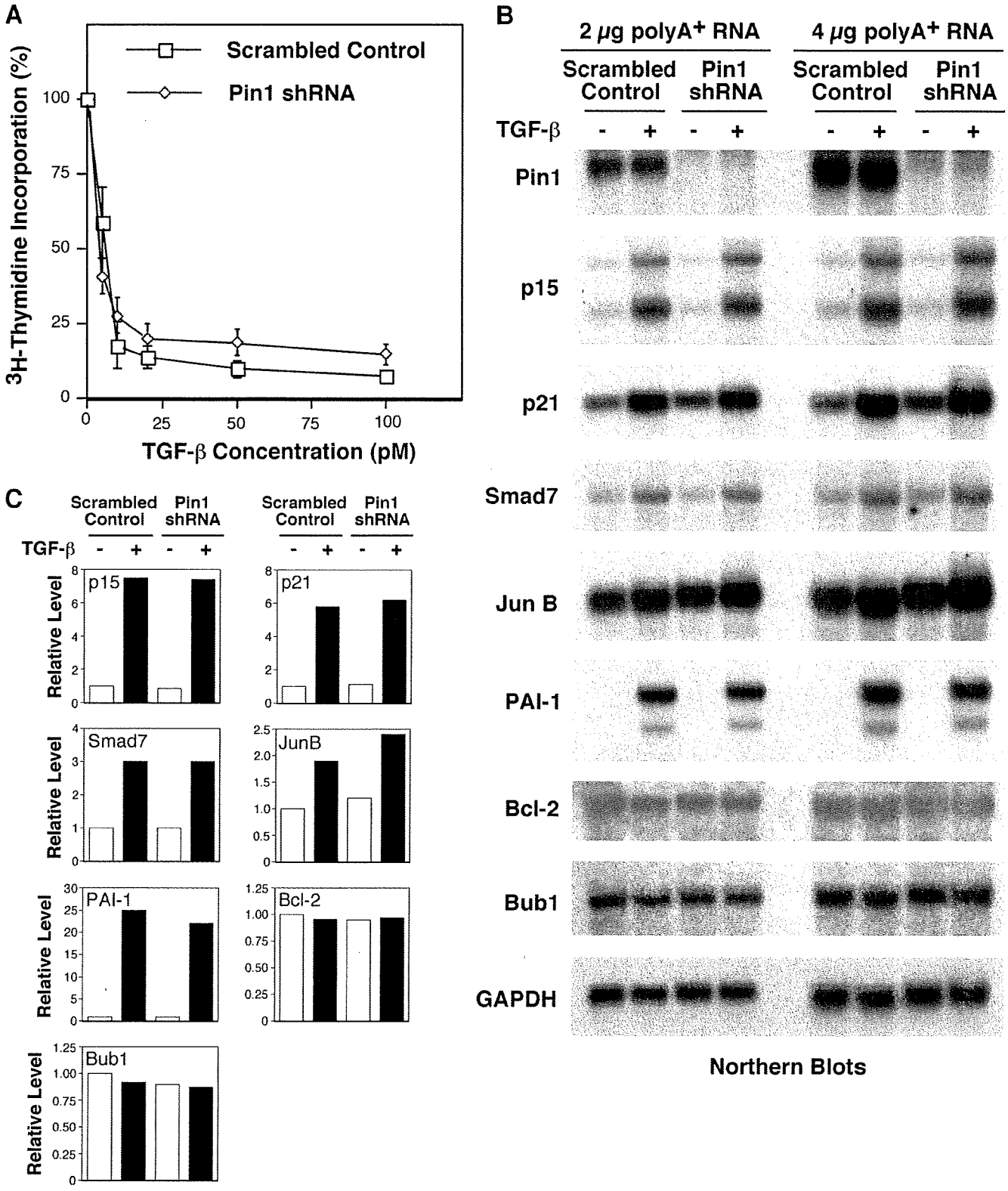

FIGURE 4. **Knockdown of Pin1 does not have a significant effect on TGF-β-induced growth-inhibitory effects.** *A*, knockdown of Pin1 does not have a significant effect on TGF-β-induced growth-inhibitory effects. Pin1 knockdown HaCaT cells and the scrambled control HaCaT cells were treated with or without TGF-β at various concentrations and then subjected to [^{3}H]thymidine incorporation assay. The results represent the average of three independent experiments. *B*, knockdown of Pin1 does not have a significant effect on several TGF-β/Smad target genes. Pin1 knockdown HaCaT cells and the scrambled control HaCaT cells were treated with or without TGF-β for 8 h. The expression levels of Pin1 and several TGF-β/Smad target genes were analyzed by Northern blot analysis as indicated. GAPDH expression levels were also analyzed as a loading control. *C*, the mRNA levels of p15, p21, Smad7, JunB, PAI-1, Bcl-2, and Bub1 in B were quantified by densitometer and normalized to GAPDH mRNA levels. The *bar graphs* represent the average of results from 2 μg of poly(A)$^+$ RNA and 4 μg of poly(A)$^+$ RNA.

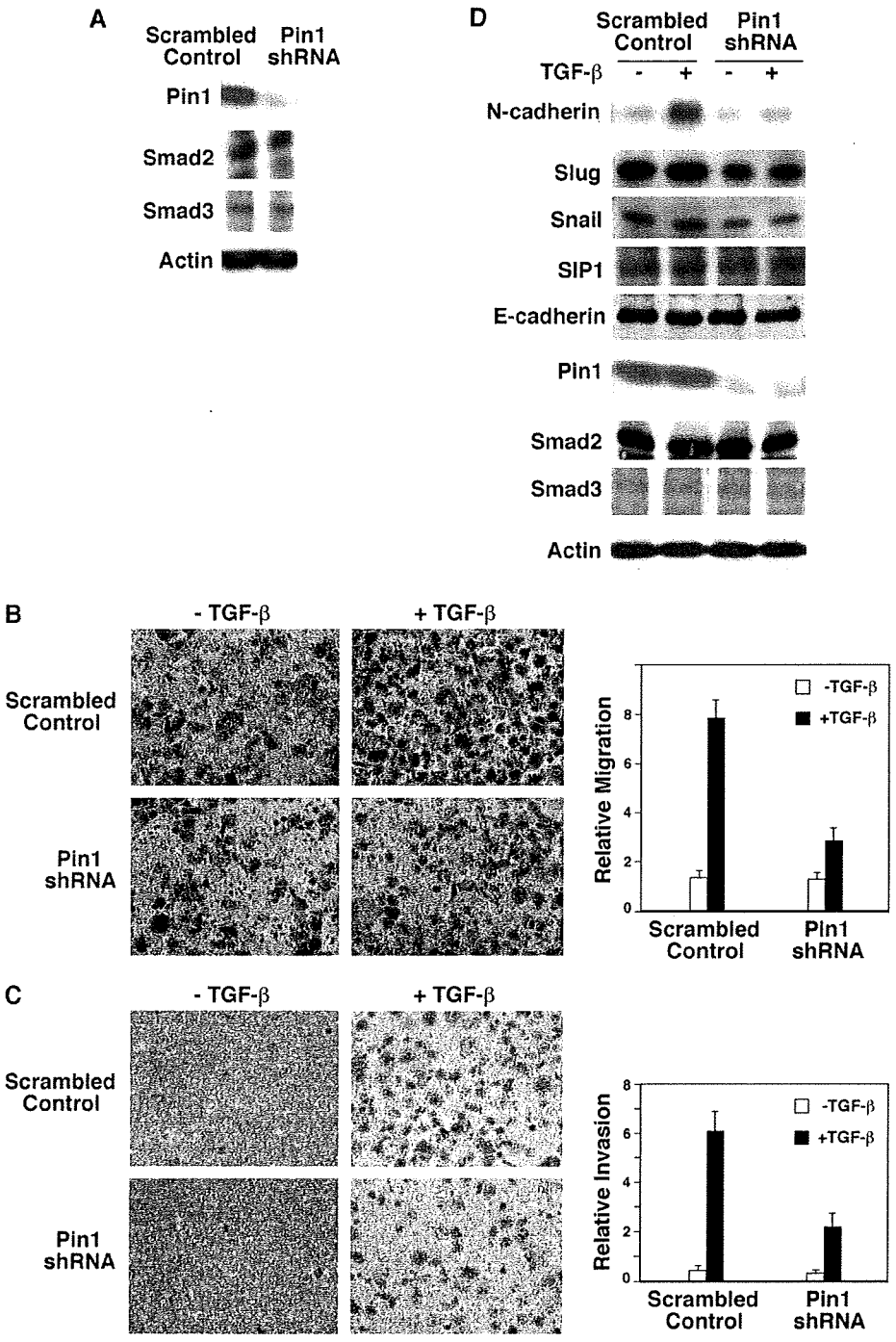

FIGURE 5. **Knockdown of Pin1 significantly reduces TGF-β-induced migration and invasion.** *A*, knockdown of Pin1 has little effect on Smad2/3 levels in the PC3 prostate cancer cells. Stable PC3 prostate cancer cell lines with the shRNA targeting Pin1 or the scrambled control were generated. The cell lysates were analyzed for expression levels of Pin1, Smad2, and Smad3. Actin levels were also analyzed as a loading control. *B*, knockdown of Pin1 significantly reduces TGF-β-induced migration of prostate cancer cells. The Pin1 knockdown PC3 cells and the scrambled control PC3 cells were subjected to the migration assay in the absence or presence of TGF-β. Representative photos of migrated cells were shown. The results from four independent experiments were plotted. *C*, knockdown of Pin1 significantly reduces TGF-β-induced invasion of prostate cancer cells. The Pin1 knockdown PC3 cells and the scrambled control PC3 cells were subjected to the invasion assay in the absence or presence of TGF-β. Representative photos of the invasion assay were shown. The results from four independent experiments were plotted. *D*, knockdown of Pin1 significantly reduces TGF-β induction of N-cadherin expression. The Pin1 knockdown PC3 cells and the scrambled control PC3 cells were treated with or without TGF-β. The cell lysates were analyzed by immunoblot with antibodies against N-cadherin, Slug, Snail, SIP1, E-cadherin, Pin1, Smad2, Smad3, and actin.

TGF-β/Smad3 in hepatocytes (70). As shown in Fig. 4, *B* and *C*, the Bcl2 levels are little affected by TGF-β treatment in the control HaCaT or Pin1 knockdown HaCaT cells, and the Bcl2 levels are very similar between the control cells and the Pin1 knockdown cells. Our previous unpublished results from a subtractive screen suggested that the expression level of Bub1, which regulates the spindle checkpoint function, was slightly reduced in response to TGF-β. We therefore also analyzed Bub1 in the Northern blot analysis. As shown in Fig. 4, *B* and *C*, the expression of Bub1 was slightly reduced in response to TGF-β in both the control cells and the Pin1 knockdown cells. The Bub1 levels at the basal state as well as after TGF-β treatment were modestly reduced in the Pin1 knockdown cells compared with the control cells. The GAPDH levels were also analyzed as a loading control (Fig. 4*B*). Taken together, the results in Fig. 4, *B* and *C*, support the notion that Pin1 does not have a significant effect on TGF-β-mediated growth-inhibitory responses.

Pin1 Promotes TGF-β-mediated Migration and Invasion—Pin1 expression is highly elevated in many cancers (39–51). Based on this notion, we next sought the possible role of Pin1 in TGF-β signaling in cancer cells. TGF-β often promotes cancer cell migration and invasion. We transduced human PC3 prostate cancer cell line with the same shRNA against Pin1 or the scrambled control as used for HaCaT cells. As shown in Fig. 5*A*, Pin1 was also effectively depleted in PC3 cells. Pin1 depletion had little effect on the Smad2 or Smad3 protein levels (Fig. 5*A*). TGF-β-mediated growth-inhibitory response was lost in this cell line (data not shown). On the other hand, TGF-β treatment of the scrambled control PC3 cells greatly stimulated their motility as analyzed in the migration assay (Fig. 5*B*). In the same assay, however, the TGF-β induction of cell motility was significantly reduced when Pin1 was depleted (Fig. 5*B*). Similarly, the

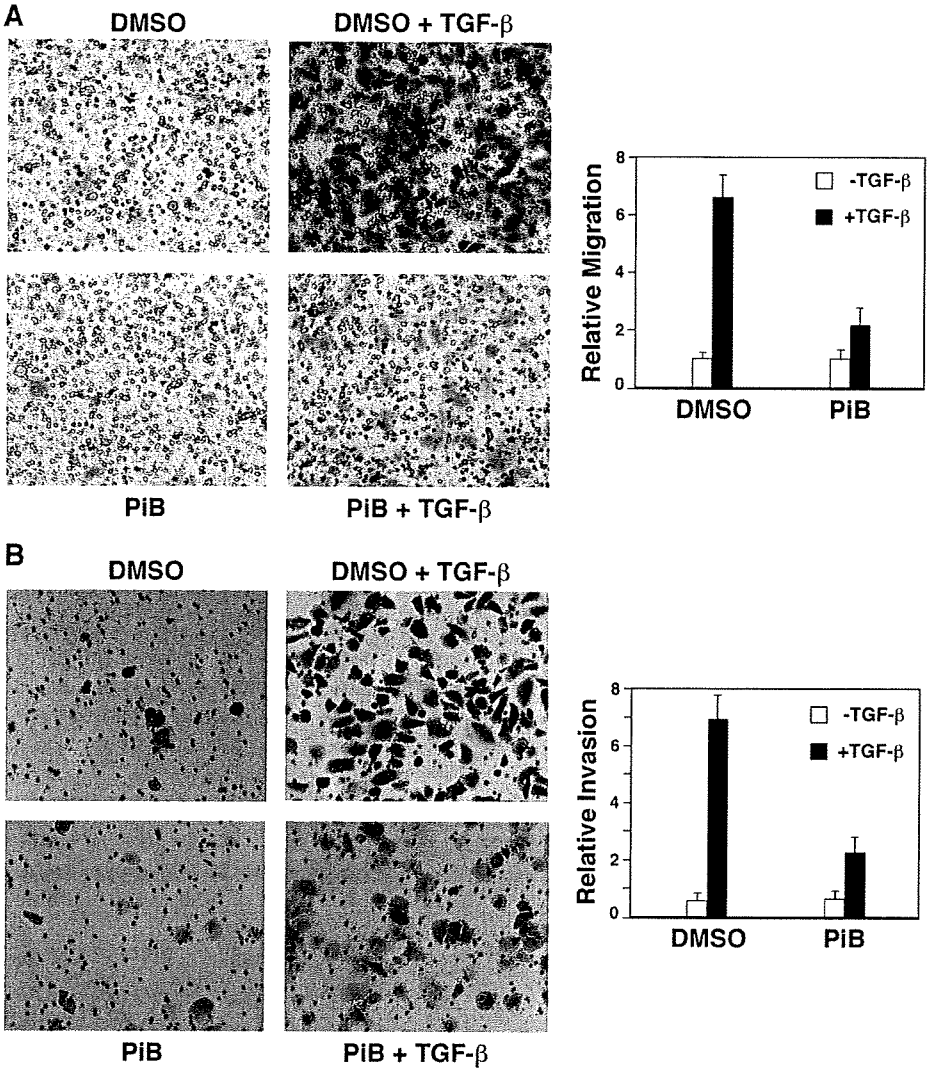

FIGURE 6. **The catalytic activity of Pin1 is necessary for TGF-β-induced migration and invasion.** *A*, the catalytic activity of Pin1 is necessary for TGF-β-induced migration. PC3 cells were subjected to the migration assay in the presence of 1 μM Pin1 inhibitor PiB or the vehicle DMSO control. Cells were treated with or without TGF-β. Representative photos of migrated cells were shown. The results from four independent experiments were plotted. *B*, catalytic activity of Pin1 is necessary for TGF-β-induced invasion. PC3 cells were subjected to the invasion assay in the presence of 1 μM PiB or the vehicle DMSO control. Cells were treated with or without TGF-β. Representative photos of the invasion assay are shown. The results from four independent experiments are plotted.

TGF-β-induced invasion was also significantly reduced in the Pin1 knockdown cells compared with the scrambled control cells (Fig. 5*C*). Thus, Pin1 promotes TGF-β-mediated migratory and invasive responses in the prostate cancer cells. Similar results were also obtained in the MDA-MB-231 breast cancer cells (data not shown). Concomitant with the TGF-β-stimulated migratory and invasive responses in the control PC3 cells, N-cadherin, an important factor for cell migration and invasion (71–77), was up-regulated by TGF-β (Fig. 5*D*). In the Pin1 depleted cells, this up-regulation was greatly reduced (Fig. 5*D*). Thus, the significantly diminished TGF-β-induced cell migration and invasion in the Pin1 knockdown cells was correlated with the greatly reduced expression of N-cadherin.

We also analyzed whether knockdown of Pin1 affects the expression levels of several epithelial mesenchymal transition-related proteins, including Slug, Snail, SIP, and E-cadherin (78–80). As shown in Fig. 5*D*, the expression of Slug and Snail was slightly increased in the presence of TGF-β. Pin1 knockdown reduced the expression of Slug and Snail. However, this effect was not dependent on TGF-β. The expression of SIP1 was slightly increased in the presence of TGF-β (Fig. 5*D*); knockdown of Pin1 had no effect on SIP1 levels in the absence or presence of TGF-β (Fig. 5*D*). The expression of E-cadherin was slightly reduced in the presence of TGF-β (Fig. 5*D*); depletion of Pin1 had no effect on E-cadherin levels in the absence or presence of TGF-β (Fig. 5*D*). These results suggest that these four proteins may not be responsible for the effect of Pin1 in TGF-β-induced migration and invasion.

The Catalytic Activity of Pin1 Is Necessary for TGF-β-induced Migration and Invasion—We next analyzed whether the peptidyl-prolyl cis/trans isomerase activity of Pin1 is necessary for TGF-β-mediated migration and invasion. PiB is a small molecule chemical inhibitor that potently and selectively inhibits Pin1/Par14 isomerase activity through competitively binding to the active site (81–83). PC3 cell migration and invasion assays were performed in the presence of 1 μM PiB or in the presence of the vehicle DMSO, which was used to dissolve PiB. Cells were treated with or without TGF-β. As shown in Fig. 6*A*, PiB significantly inhibited TGF-β-induced migration. Similarly, PiB also significantly inhibited TGF-β-mediated invasion (Fig. 6*B*). Thus, we conclude that the catalytic activity of Pin1 is necessary for its effect in TGF-β-induced migration and invasion.

DISCUSSION

Pin1 is a peptidyl-prolyl cis/trans isomerase that recognizes a small subset of the phosphorylated serine/threonine-proline motifs (39–41). We show in this report that Pin1 binds to Smad2/3 in response to TGF-β. Depletion of Pin1 does not have a significant effect on the Smad2/3 levels as analyzed in the human HaCaT keratinocytes and the human PC3 prostate cancer cells. We further show that the phosphorylated Thr-179-proline motif in the Smad3 linker region is the major binding site for Pin1 after TGF-β treatment and suggest that C-tail

phosphorylation is necessary for association with Pin1. Pin1 binding does not have a significant effect on the phosphorylation levels of Thr-179 or the other sites in the linker region of Smad3 in response to TGF-β. Depletion of Pin1 does not have a significant effect on the TGF-β-induced growth-inhibitory responses. In contrast, depletion of Pin1 markedly reduces TGF-β-induced prostate cancer cell migration and invasion. Similar results were also obtained in the MDA-MB-231 breast cancer cells (data not shown). We conclude that Pin1 promotes TGF-β-mediated migration and invasion.

A recent study by Nakano *et al.* (53) reported that Pin1 enhances Smurf2 interaction with Smad2/3 and leads to decreased levels of Smad2/3. This study showed that knockdown of Pin1 increased Smad2/3 protein levels in the MDA-MB-231 breast cancer cell line (53). Overall, the effect of Pin1 on Smad2/3 protein levels was relatively modest, as quantified in this study. We detected little difference in the Smad2/3 levels in the HaCaT keratinocytes and the PC3 prostate cancer cells when Pin1 was very effectively depleted. One possibility is that the relatively modest Pin1- and Smurf2-dependent degradation of Smad2/3 is cell type-dependent. Previous studies have shown that although Smurf2 binds to Smad3, it does not degrade Smad3 (84, 85). These observations are consistent with the idea of cell-type specificity.

We have shown in this study that Smad2/3 interaction with Pin1 is specific in response to TGF-β. Although EGF induces phosphorylation of the same linker sites as TGF-β to a similar extent, EGF has little effect in inducing Pin1 interaction with Smad2/3. Analysis of the Smad3 mutant at the C-tail phosphorylation sites suggests that the C-tail phosphorylation is necessary for Pin1 binding. The study by Nakano *et al.* (53) showed that a constitutively activated Ras, which leads to Smad2/3 phosphorylation in the linker region, can also induce Smad2/3 binding to Pin1. In addition to activating ERK, which phosphorylates Smad2/3 in the linker region, Ras may have other functions in terms of regulating Smad2/3 phosphorylation. A previous study has shown that Mps1, a dual specificity protein kinase for spindle checkpoint function, can phosphorylate Smad2/3 at the C-tail SS*X*S motif independent of TGF-β signaling (86). Interestingly, a study showed that constitutively activated B-Raf increased Mps1 protein level and activity (87). Thus, it is possible that the constitutively activated Ras can increase the Mps1 activity, leading to the C-tail phosphorylation of Smad2/3. Both the C-tail and linker phosphorylated Smad2/3 then interact with Pin1. In any case, Pin1 binds to Smad2/3 to a much greater extent in response to TGF-β than in response to the activated Ras (53), indicating the importance of TGF-β in regulating the interaction between Smad2/3 and Pin1.

We have shown in this study that the Thr-179 in the Smad3 linker region plays a major role in the interaction with Pin1 in response to TGF-β. When the Thr-179 site was mutated, Smad3 association with Pin1 was dramatically reduced. This result suggests that Pin1 and Smad3 interact at 1:1 ratio. The recent study by Nakano *et al.* (53) showed that mutation of all four sites in the Smad3 linker region was necessary to disrupt Smad3-Pin1 interaction. Careful analysis of their data, taken into the consideration of the input protein levels, would also suggest that Thr-179 is the major binding site for Smad3 to interact with Pin1.

We analyzed several TGF-β-mediated responses in our studies. Depletion of Pin1 does not have a significant effect on the TGF-β growth-inhibitory responses. We have also analyzed whether depletion of Pin1 affected TGF-β-induced epithelial mesenchymal transition in the PC3 prostate cancer cells, and our studies suggest that depletion of Pin1 modestly reduced TGF-β-mediated epithelial mesenchymal transition in the PC3 cells (data not shown). Thus, Pin1 has a specific role in promoting migration and invasion in response to TGF-β.

The effect of Pin1 in TGF-β-induced migration and invasion is accompanied with the regulation of the expression of N-cadherin, which plays an important role in migration and invasion (71–77), including in the PC3 prostate cancer cells (75). N-cadherin protein levels are induced by TGF-β treatment. When Pin1 is depleted, the TGF-β induction of N-cadherin is dramatically reduced. Analysis of the N-cadherin promoter sequence *in silico* indicates that it contains a consensus Smad binding element, suggesting that Smad proteins may directly bind to its promoter and regulate its expression. Pin1 can induce conformational changes of a number of its substrates (39–41). This can lead to increased protein stability, decreased protein stability, altered transcriptional activity, or other effects (39–41). The effect of Pin1 on TGF-β/Smad target genes varies. For example, Pin1 essentially has no effect on the p15, p21, and Smad7 levels, has a modest inhibitory effect on JunB, has a modest stimulatory effect on PAI-1, and has a significant stimulatory effect on N-cadherin. Thus, the effect of Pin1 on the TGF-β/Smad target genes appears to depend on the promoter context.

Pin1 is overexpressed in many cancers (39–51). Among 60 different tumor types analyzed, 38 tumor types have Pin1 overexpression in 10% to nearly 100% of the cases analyzed, such as prostate, breast, lung, colon, ovary, cervical, brain tumors, and melanoma (44). Thus, Pin1 overexpression is a specific and prevalent event in human cancers. Previous studies have shown that Pin1 is an excellent prognostic marker in prostate cancer (52), the most common cancer in men in the United States. Patients with higher expression of Pin1 have a significantly higher probability of recurrence than patients with low expression of Pin1. In addition, patients with a high expression of Pin1 have almost four times the risk of having earlier recurrence than those patients with low expression of Pin1. Furthermore, patients with a very high level of Pin1 have more than eight times the risk of having earlier recurrence than the patients with a low level of Pin1 (52). TGF-β promotes cancer progression and metastasis. We have shown in this report that Pin1 mediates TGF-β-induced migration and invasion of prostate cancer cells. Pin1 can also promote migration and invasion at basal state (55). Our findings highlight the importance of Pin1 in cancer progression and metastasis, especially for prostate cancer. Furthermore, our findings highly suggest that Pin1 is an important therapeutic target for prostate cancer, breast cancer, and some other types of cancers.

Acknowledgments—We are very grateful to K. Liang for generous help with this project, to L.-H. Wang and members of his laboratory, especially S.-H. Chan, for assisting the migration and invasion assays and for discussions, to E. B. Leof for the Smad3 C-tail phosphopeptide antibody, and to G. Fan, P. Molli, X. Zheng, C. Chu, I. M. Liu, C. Lu, K.-T. Lin, and C. Gelinas for assistance and helpful discussions.

REFERENCES

1. Roberts, A. B., and Sporn, M. B. (1990) in *Peptide Growth Factors and Their Receptors* (Sporn, M. B., and Roberts, A. B., eds) pp. 419–472, Springer-Verlag, Heidelberg, Germany
2. Massagué, J., Blain, S. W., and Lo, R. S. (2000) *Cell* **103,** 295–309
3. Derynck, R., Akhurst, R. J., and Balmain, A. (2001) *Nat. Genet.* **29,** 117–129
4. Roberts, A. B., and Wakefield, L. M. (2003) *Proc. Natl. Acad. Sci. U.S.A.* **100,** 8621–8623
5. Miyazono, K., Suzuki, H., and Imamura, T. (2003) *Cancer Sci.* **94,** 230–234
6. Levy, L., and Hill, C. S. (2006) *Cytokine Growth Factor Rev.* **17,** 41–58
7. Massagué, J. (2008) *Cell* **134,** 215–230
8. Pardali, E., and ten Dijke, P. (2009) *Front. Biosci.* **14,** 4848–4861
9. Heldin, C. H., Miyazono, K., and ten Dijke, P. (1997) *Nature* **390,** 465–471
10. Shi, Y., and Massagué, J. (2003) *Cell* **113,** 685–700
11. Derynck, R., and Zhang, Y. E. (2003) *Nature* **425,** 577–584
12. Liu, F. (2003) *Front. Biosci.* **8,** s1280–1303
13. ten Dijke, P., and Hill, C. S. (2004) *Trends Biochem. Sci.* **29,** 265–273
14. Feng, X. H., and Derynck, R. (2005) *Annu. Rev. Cell Dev. Biol.* **21,** 659–693
15. de Caestecker, M. P., Parks, W. T., Frank, C. J., Castagnino, P., Bottaro, D. P., Roberts, A. B., and Lechleider, R. J. (1998) *Genes Dev.* **12,** 1587–1592
16. Engel, M. E., McDonnell, M. A., Law, B. K., and Moses, H. L. (1999) *J. Biol. Chem.* **274,** 37413–37420
17. Kretzschmar, M., Doody, J., Timokhina, I., and Massagué, J. (1999) *Genes Dev.* **13,** 804–816
18. Hu, P. P., Shen, X., Huang, D., Liu, Y., Counter, C., and Wang, X. F. (1999) *J. Biol. Chem.* **274,** 35381–35387
19. Lehmann, K., Janda, E., Pierreux, C. E., Rytömaa, M., Schulze, A., McMahon, M., Hill, C. S., Beug, H., and Downward, J. (2000) *Genes Dev.* **14,** 2610–2622
20. Blanchette, F., Rivard, N., Rudd, P., Grondin, F., Attisano, L., and Dubois, C. M. (2001) *J. Biol. Chem.* **276,** 33986–33994
21. Attisano, L., and Wrana, J. L. (2002) *Science* **296,** 1646–1647
22. Grimm, O. H., and Gurdon, J. B. (2002) *Nat. Cell Biol.* **4,** 519–522
23. Funaba, M., Zimmerman, C. M., and Mathews, L. S. (2002) *J. Biol. Chem.* **277,** 41361–41368
24. Massague, J. (2003) *Genes Dev.* **17,** 2993–2997
25. Furukawa, F., Matsuzaki, K., Mori, S., Tahashi, Y., Yoshida, K., Sugano, Y., Yamagata, H., Matsushita, M., Seki, T., Inagaki, Y., Nishizawa, M., Fujisawa, J., and Inoue, K. (2003) *Hepatology* **38,** 879–889
26. Matsuura, I., Denissova, N. G., Wang, G., He, D., Long, J., and Liu, F. (2004) *Nature* **430,** 226–231
27. Liu, F., and Matsuura, I. (2005) *Cell Cycle* **4,** 63–66
28. Liu, F. (2006) *Cytokine Growth Factor Rev.* **17,** 9–17
29. Matsuura, I., Wang, G., He, D., and Liu, F. (2005) *Biochemistry* **44,** 12546–12553
30. Mori, S., Matsuzaki, K., Yoshida, K., Furukawa, F., Tahashi, Y., Yamagata, H., Sekimoto, G., Seki, T., Matsui, H., Nishizawa, M., Fujisawa, J., and Okazaki, K. (2004) *Oncogene* **23,** 7416–7429
31. Yamagata, H., Matsuzaki, K., Mori, S., Yoshida, K., Tahashi, Y., Furukawa, F., Sekimoto, G., Watanabe, T., Uemura, Y., Sakaida, N., Yoshioka, K., Kamiyama, Y., Seki, T., and Okazaki, K. (2005) *Cancer Res.* **65,** 157–165
32. Kamaraju, A. K., and Roberts, A. B. (2005) *J. Biol. Chem.* **280,** 1024–1036
33. Javelaud, D., and Mauviel, A. (2005) *Oncogene* **24,** 5742–5750
34. Sapkota, G., Alarcón, C., Spagnoli, F. M., Brivanlou, A. H., and Massagué, J. (2007) *Mol. Cell* **25,** 441–454
35. Guo, X., Ramirez, A., Waddell, D. S., Li, Z., Liu, X., and Wang, X. F. (2008) *Genes Dev.* **22,** 106–120
36. Wang, G., Matsuura, I., He, D., and Liu, F. (2009) *J. Biol. Chem.* **284,** 9663–9673
37. Millet, C., Yamashita, M., Heller, M., Yu, L. R., Veenstra, T. D., and Zhang, Y. E. (2009) *J. Biol. Chem.* **284,** 19808–19816
38. Matsuzaki, K., Kitano, C., Murata, M., Sekimoto, G., Yoshida, K., Uemura, Y., Seki, T., Taketani, S., Fujisawa, J., and Okazaki, K. (2009) *Cancer Res.* **69,** 5321–5330
39. Lu, K. P., and Zhou, X. Z. (2007) *Nat. Rev. Mol. Cell Biol.* **8,** 904–916
40. Yeh, E. S., and Means, A. R. (2007) *Nat. Rev. Cancer.* **7,** 381–388
41. Takahashi, K., Uchida, C., Shin, R. W., Shimazaki, K., and Uchida, T. (2008) *Cell. Mol. Life Sci.* **65,** 359–375
42. Wulf, G. M., Ryo, A., Wulf, G. G., Lee, S. W., Niu, T., Petkova, V., and Lu, K. P. (2001) *EMBO J.* **20,** 3459–3472
43. Ryo, A., Nakamura, M., Wulf, G., Liou, Y. C., and Lu, K. P. (2001) *Nat. Cell Biol.* **3,** 793–801
44. Bao, L., Kimzey, A., Sauter, G., Sowadski, J. M., Lu, K. P., and Wang, D. G. (2004) *Am. J. Pathol.* **164,** 1727–1737
45. He, J., Zhou, F., Shao, K., Hang, J., Wang, H., Rayburn, E., Xiao, Z. X., Lee, S. W., Xue, Q., Feng, X. L., Shi, S. S., Zhang, C. Y., and Zhang, S. (2007) *Lung Cancer* **56,** 51–58
46. Kim, C. J., Cho, Y. G., Park, Y. G., Nam, S. W., Kim, S. Y., Lee, S. H., Yoo, N. J., Lee, J. Y., and Park, W. S. (2005) *World J. Gastroenterol.* **11,** 5006–5009
47. Pang, R., Yuen, J., Yuen, M. F., Lai, C. L., Lee, T. K., Man, K., Poon, R. T., Fan, S. T., Wong, C. M., Ng, I. O., Kwong, Y. L., and Tse, E. (2004) *Oncogene* **23,** 4182–4186
48. Pang, R. W., Lee, T. K., Man, K., Poon, R. T., Fan, S. T., Kwong, Y. L., and Tse, E. (2006) *J. Pathol.* **210,** 19–25
49. Chen, S. Y., Wulf, G., Zhou, X. Z., Rubin, M. A., Lu, K. P., and Balk, S. P. (2006) *Mol. Cell. Biol.* **26,** 929–939
50. Lam, P. B., Burga, L. N., Wu, B. P., Hofstatter, E. W., Lu, K. P., and Wulf, G. M. (2008) *Mol. Cancer* **7,** 91
51. Fan, G., Fan, Y., Gupta, N., Matsuura, I., Liu, F., Zhou, X. Z., Lu, K. P., and Gélinas, C. (2009) *Cancer Res.* **69,** 4589–4597
52. Ayala, G., Wang, D., Wulf, G., Frolov, A., Li, R., Sowadski, J., Wheeler, T. M., Lu, K. P., and Bao, L. (2003) *Cancer Res.* **63,** 6244–6251
53. Nakano, A., Koinuma, D., Miyazawa, K., Uchida, T., Saitoh, M., Kawabata, M., Hanai, J., Akiyama, H., Abe, M., Miyazono, K., Matsumoto, T., and Imamura, T. (2009) *J. Biol. Chem.* **284,** 6109–6115
54. Yaffe, M. B., Schutkowski, M., Shen, M., Zhou, X. Z., Stukenberg, P. T., Rahfeld, J. U., Xu, J., Kuang, J., Kirschner, M. W., Fischer, G., Cantley, L. C., and Lu, K. P. (1997) *Science* **278,** 1957–1960
55. Ryo, A., Uemura, H., Ishiguro, H., Saitoh, T., Yamaguchi, A., Perrem, K., Kubota, Y., Lu, K. P., and Aoki, I. (2005) *Clin. Cancer Res.* **11,** 7523–7531
56. Denissova, N. G., Pouponnot, C., Long, J., He, D., and Liu, F. (2000) *Proc. Natl. Acad. Sci. U.S.A.* **97,** 6397–6402
57. Sachdev, P., Zeng, L., and Wang, L. H. (2002) *J. Biol. Chem.* **277,** 17638–17648
58. Cheng, G. Z., Chan, J., Wang, Q., Zhang, W., Sun, C. D., and Wang, L. H. (2007) *Cancer Res.* **67,** 1979–1987
59. Lu, K. P., Hanes, S. D., and Hunter, T. (1996) *Nature* **380,** 544–547
60. Hannon, G. J., and Beach, D. (1994) *Nature* **371,** 257–261
61. Datto, M. B., Li, Y., Panus, J. F., Howe, D. J., Xiong, Y., and Wang, X. F. (1995) *Proc. Natl. Acad. Sci. U.S.A.* **92,** 5545–5549
62. Feng, X. H., Lin, X., and Derynck, R. (2000) *EMBO J.* **19,** 5178–5193
63. Moustakas, A., and Kardassis, D. (1998) *Proc. Natl. Acad. Sci. U.S.A.* **95,** 6733–6738
64. Pardali, K., Kurisaki, A., Morén, A., ten Dijke, P., Kardassis, D., and Moustakas, A. (2000) *J. Biol. Chem.* **275,** 29244–29256
65. Seoane, J., Le, H. V., Shen, L., Anderson, S. A., and Massagué, J. (2004) *Cell* **117,** 211–223
66. Nagarajan, R. P., Zhang, J., Li, W., and Chen, Y. (1999) *J. Biol. Chem.* **274,** 33412–33418
67. Jonk, L. J., Itoh, S., Heldin, C. H., ten Dijke, P., and Kruijer, W. (1998) *J. Biol. Chem.* **273,** 21145–21152
68. López-Rovira, T., Chalaux, E., Rosa, J. L., Bartrons, R., and Ventura, F. (2000) *J. Biol. Chem.* **275,** 28937–28946
69. Dennler, S., Itoh, S., Vivien, D., ten Dijke, P., Huet, S., and Gauthier, J. M. (1998) *EMBO J.* **17,** 3091–3100
70. Yang, Y. A., Zhang, G. M., Feigenbaum, L., and Zhang, Y. E. (2006) *Cancer Cell* **9,** 445–457
71. Behrens, J. (1993) *Breast Cancer Res. Treat.* **24,** 175–184
72. Gumbiner, B. M. (1996) *Cell* **84,** 345–357
73. Price, J. T., Bonovich, M. T., and Kohn, E. C. (1997) *Crit. Rev. Biochem. Mol. Biol.* **32,** 175–253
74. Derycke, L. D., and Bracke, M. E. (2004) *Int. J. Dev. Biol.* **48,** 463–476
75. Alexander, N. R., Tran, N. L., Rekapally, H., Summers, C. E., Glackin, C., and Heimark, R. L. (2006) *Cancer Res.* **66,** 3365–3369
76. Mariotti, A., Perotti, A., Sessa, C., and Rüegg, C. (2007) *Expert Opin. In-*